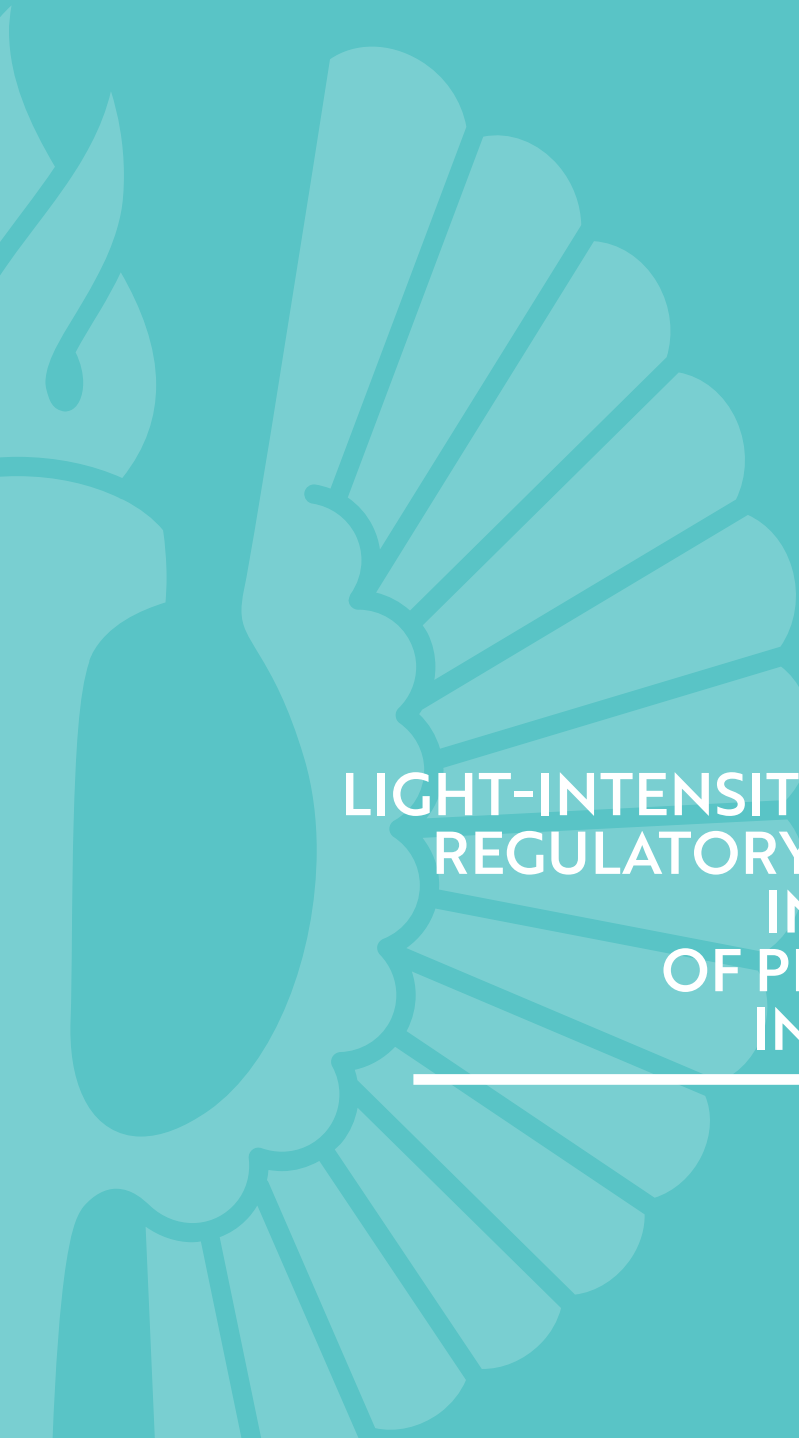




UNIVERSITY  
OF TURKU

A large, faint, light-teal illustration of a sunflower is positioned on the left side of the cover, partially overlapping the title text.

# LIGHT-INTENSITY-DEPENDENT REGULATORY MECHANISMS IN PROTECTION OF PHOTOSYSTEM I IN ARABIDOPSIS

---

Sanna Rantala





UNIVERSITY  
OF TURKU

# **LIGHT-INTENSITY-DEPENDENT REGULATORY MECHANISMS IN PROTECTION OF PHOTOSYSTEM I IN ARABIDOPSIS**

---

Sanna Rantala

## University of Turku

---

Faculty of Science and Engineering  
Department of Biochemistry  
Molecular Plant Biology  
Doctoral Programme in Molecular  
Life Sciences

### Supervised by

---

Professor Eva-Mari Aro  
Molecular Plant Biology  
Department of Biochemistry  
University of Turku  
Finland

Assistant Professor Mikko Tikkanen  
Molecular Plant Biology  
Department of Biochemistry  
University of Turku  
Finland

Doctor Arjun Tiwari  
Molecular Plant Biology  
Department of Biochemistry  
University of Turku  
Finland

### Reviewed by

---

Professor Janne Ihalainen  
Department of Biological and  
Environmental Science  
University of Jyväskylä  
Finland

Associate Professor Albert Porcar-Castell  
Department of Forest Sciences  
University of Helsinki  
Finland

### Opponent

---

Professor Győző Garab  
Biological Research Centre  
Hungarian Academy of Sciences  
Hungary

The originality of this publication has been checked in accordance with the University of Turku quality assurance system using the Turnitin OriginalityCheck service.

ISBN 978-951-29-7734-5 (PRINT)  
ISBN 978-951-29-7735-2 (PDF)  
ISSN 0082-7002 (Print)  
ISSN 2343-3175 (Online)  
Grano Oy - Turku, Finland 2019

TURUN YLIOPISTO

Luonnontieteiden ja tekniikan tiedekunta

Biokemian laitos

Molekulaarinen kasvibiologia

SANNA RANTALA: Light-intensity-dependent regulatory mechanisms in protection of Photosystem I in *Arabidopsis*

Väitöskirja, 116 s.

Molekulaaristen biotieteiden tohtoriohjelma

Heinäkuu 2019

## Tiivistelmä

Fotosynteesin valoreaktioissa viherhiukkasen tylakoidikalvoon sitoutuneet fotosysteemi (PS)II ja PSI sekä Sytokromi  $b_6/f$  siirtävät elektroneja vesimolekyyliltä  $NADP^+$ :lle pääasiassa valoahaavikompleksien (LHC)II ja LHCI keräämän valoenergian avulla. Samalla tylakoidikalvolle muodostuu elektrokemiallinen gradientti, jonka avulla ATP-syntaasi katalysoi ATP:n muodostumista. Valoreaktioiden lopputuotteita, NADPH:ta ja ATP:ta, kasvi käyttää sitoakseen ilmakehän hiilidioksidia eloperäisiksi yhdisteiksi, jotka ylläpitävät paitsi kasvien kasvua ja kehitystä, myös lähes kaikkea Maan toisenvaraista elämää. Elektronien kulkua valoreaktioissa on ohjattava tarkoin, jotteivät ne vaurioita PSI:tä, jota varten ei ole kehittynyt tehokasta korjauskiertoa kuten PSII:lla. PSI:n suojaamiseksi kasvit kykenevät säätelemään valoenergian jakautumista fotosysteemien välillä fosforyloimalla ja defosforyloimalla LHCI:ta, optimoimaan elektronien kulkunopeutta PSII:lta PSI:lle PGR5-proteiinin avulla sekä kierrättämään elektroneja PSI:ltä takaisin elektroninsiirtoketjuun NDH-1-kompleksin kautta. Tässä väitöskirjaprojektissa vertailin biokemiallisin ja biofysikaalisin menetelmin lituruohon *Arabidopsis thaliana* villityyppejä ja mutanttilinjoja, joilta on poistettu tunnettu säätelyproteiini. Osoitin, että LHCI:n defosforylaatio suojaa kirkkaassa valossa PSI:tä liiallisilta elektroneilta erottamalla kompleksit fyysisesti toisistaan, mutta säätelee myös Sytokromi  $b_6/f$ :n ja ATP-syntaasin sijaintia tylakoidikalvolla. Osoitin myös, että PGR5-proteiini aktivoituu valossa ja kontrolloi elektroninsiirtoa PSII:lta PSI:lle, mutta ei PSI:ltä eteenpäin. Lisäksi havainnollistin, että mikäli PSI kuitenkin vahingoittuu, sekä PGR5 että NDH-1 osallistuvat fotosynteettisen elektroninsiirtoketjun toiminnan säilyttämiseen.

Avainsanat: fotosynteesi, valoreaktiot, LHCI, fotoinhibitio, fosforylaatio, digitoniini, fluoresenssi, STN7, TAP38/PPH1, PGR5, NDH-1, PTOX

UNIVERSITY OF TURKU

Faculty of Science and Engineering

Department of Biochemistry

Molecular Plant Biology

SANNA RANTALA: Light-intensity-dependent regulatory mechanisms in protection of Photosystem I in *Arabidopsis*

Doctoral Dissertation, 116 pp.

Doctoral Programme in Molecular Life Sciences

July 2019

## Abstract

In photosynthetic light reactions, photosystem (PS)II and PSI as well as Cytochrome  $b_6/f$ , which are embedded in the thylakoid membrane of chloroplasts, transfer electrons from water molecules to  $NADP^+$  using the light energy collected mostly by light harvesting complexes (LHC)II and LHCI. Simultaneously, an electrochemical gradient is formed across the thylakoid membrane and utilized by ATP synthase to catalyse the synthesis of ATP. With the end products of photosynthetic light reactions, NADPH and ATP, plants bind atmospheric carbon dioxide into organic compounds, which not only support the plants' growth and development but also nearly all heterotrophic life on Earth. The flow of electrons in the photosynthetic machinery needs to be strictly controlled in order to avoid damage to PSI that, unlike PSII, lacks an efficient repair cycle. To protect PSI, plants are able to control the distribution of energy between the photosystems through phosphorylating and dephosphorylating LHCII, to optimize the electron transfer rate from PSII to PSI through PGR5 protein and to cycle electrons from PSI back to the electron transfer chain through the NDH-1 complex. Here, I applied several biochemical and biophysical approaches to compare the thale cress *Arabidopsis thaliana* wild type and transgenic lines lacking certain regulatory proteins. I showed that dephosphorylation of LHCII protects PSI from excess electrons by physically separating the complexes but also by regulating the location of Cytochrome  $b_6/f$  and ATP synthase in the thylakoid membrane. Furthermore, I showed that the activation of PGR5 requires light and that when active, the protein controls electron transfer from PSII to PSI but not from PSI onwards. Finally, I demonstrated that in the case of PSI damage, both PGR5 and NDH-1 participate in maintaining the function of the photosynthetic electron transfer chain.

Keywords: photosynthesis, light reactions, LHCII, photoinhibition, phosphorylation, digitonin, fluorescence, STN7, TAP38/PPH1, PGR5, NDH-1, PTOX

# Acknowledgements

This research was funded by Academy of Finland's Centre of Excellence *Molecular Biology of Primary Producers* and Doctoral Programme in Molecular Life Sciences. I am eternally grateful to Academician Eva-Mari Aro for giving me the opportunity to work in her globally acknowledged research group under her wise supervision. I wish to express my deepest appreciation to Assistant Professor Mikko Tikkanen – his distinctive ideas and supervision were central for this work. Supervisor Doctor Arjun Tiwari is acknowledged for the inspiring lectures and enthusiastic discussions about PGR5 and PSI photoinhibition. From the bottom of my heart, I want to thank Professor Eevi Rintamäki, first, for letting me to get acquainted with plant science as a trainee in her research group in summer 2012, and, later, for the guidance during my doctoral studies. I would like to express my sincere appreciation to Associate Professor Albert Porcar-Castell and Professor Janne Ihalainen for the excellent improvements for this thesis. Henna Raudaskoski is acknowledged for her precise language check, and Doctor Caterina Gerotto, Doctor Michele Grieco, Tapio Lempiäinen and Ville Käpylä for their contribution in the Papers I, II and IV. Advisory board members Doctor Yagut Allahverdiyeva-Rinne and Doctor Mikael Brosché are thanked for the constructive criticism throughout the thesis project.

I wish to thank the entire unit of Molecular plant biology for the supportive work environment. None of this work would have been possible without the efforts of Anniina, Eve, Kurt, Maija, and Tapio R in keeping the laboratories functional. Thank you, Mika, for acquainting me with biophysics and providing humour into the everyday work. Thank you, Paula, for always finding something positive to say on my presentations. Thank you, Andrea and Pete, for the fruitful discussions. Thank you, Daniel, Jatta, Lauri, Magda, Martina A, Martina J, Minna, Moona, Sara, Steffen and Tuomas, for all the fun. Thank you, Marjaana S, Ninni and Sari, for the precious professional and nonprofessional advice. Special thanks to Vipu for the patient guidance and listening.

Support from friends and family has been crucial for this work. Thank you, Heli, Anna, Johanna, Jussi, Essi, Iris, Marianna, Paula and Mikaela, for making me celebrate the good in life every now and then. Thank you, Jyrki, for the indispensable work with Paper I, but more importantly, for the numerous prep-talks and endless

sympathy. Thank you, Aiste, for making the high pitch “believe in yourself” play in my head when I felt completely useless. Heartfelt thanks to Marjaana, for always taking the time to listen to all my problems and providing a solution or a diagnosis – I could not have done this without you. Thank you, Valtteri, Marlene and Kari, for showing interest towards my work and being proud of me. Thank you, Isä, for sparking my interest towards science. Thank you, Äiti, for teaching me that I can do anything. Finally, thank you, Andreas, for loving me even as a weepy anxious mess.

19.6.2019

*Sanna Rantala*



# List of original papers

This thesis is composed of three published articles and one submitted manuscript, collectively called papers. In the text, the papers are referred to by their Roman numerals:

- I Rantala S & Tikkanen M (2018) Light intensity- and phosphorylation-dependent rearrangements of the functional unit of photosynthetic light reactions. *Plant Direct* 2:1–12.
- II Tikkanen M, Rantala S, Grieco M, Aro EM (2017) Comparative analysis of mutant plants impaired in the main regulatory mechanisms of photosynthetic light reactions – From biophysical measurements to molecular mechanisms. *Plant Physiology and Biochemistry* 112:290–301.
- III Tikkanen M, Rantala S, Aro EM (2015) Electron flow from PSII to PSI under high light is controlled by PGR5 but not by PSBS. *Frontiers in Plant Science* 6:521.
- IV Rantala S, Tapio Lempiäinen, Caterina Gerotto, Tiwari A, Aro EM, Tikkanen M (2019) PGR5 and NDH-1 systems do not function as protective electron acceptors but mitigate the consequences of PSI inhibition. Manuscript.

Paper I is reprinted by kind permission of John Wiley & Sons, Inc.

Paper II is reprinted by kind permission of Elsevier.

Paper III is reprinted by kind permission of Frontiers Media SA.

# Table of contents

**Tiivistelmä**

**Abstract**

**Acknowledgements**

**List of original papers**

<b>1 Introduction</b>	<b>11</b>
1.1 Photosynthetic light reactions	11
1.2 Structure and interactions of the photosystems	14
1.3 Thylakoid structure and dynamics	14
1.4 Thylakoid fractionation	17
1.5 Photoinhibition of the photosystems	18
1.6 Regulation of light reactions	19
1.6.1 Phosphorylation of LHCII and PSII core proteins	19
1.6.2 Thermal dissipation of excess excitation energy from LHCII	21
1.6.3 Photosynthetic control of electron transfer through Cyt $b_6/f$ complex	21
1.6.4 NDH-1-dependent electron transfer	21
1.6.5 PGR5-dependent control of electron transfer	22
<b>2 Aims of the Study</b>	<b>23</b>
<b>3 Methodology</b>	<b>24</b>
3.1 Plant lines and their growth and treatments	24
3.2 Thylakoid isolation	25
3.3 Gradual fractionation of thylakoids with digitonin	25
3.4 Quantitating proteins with Western blotting	26
3.5 Visualizing protein complexes with blue native gel electrophoresis	26
3.6 Measuring functional photosystems with fluorescence and absorption signal	27

<b>4 Results</b>	<b>29</b>
4.1 Phosphorylation-dependent rearrangements in the PSII–LHCII–PSI–LHCI megacomplex	29
4.1.2 L-LHCII connects the differently localized photosystems	29
4.1.2 Phosphorylation status of LHCB2 determines the association of PSI in the large megacomplex at grana margins	30
4.2 Dependency of Dual-PAM parameters on light intensity and regulatory mechanisms	32
4.2.1 Biophysically determined redox state of ETC is directly dependent on the growth light intensity	32
4.2.2 Reversible phosphorylation, thermal dissipation and PGR5-dependent control optimize the redox state of ETC	33
4.2.3 PSI photoinhibition may affect the interpretation of fluorescence parameters	35
4.3 Role of PGR5 and NDH-1 in protecting PSI from photoinhibition	35
4.3.1 PGR5 and NDH-1 are unable to protect PSI by accepting electrons upon a sudden increase in light intensity	36
4.3.2 Mobile electron carriers and PGR5-dependent photosynthetic control maintain ETC after PSI photoinhibition	37
4.3.3 NDH-1 and PTOX protect PSI from over-reduction by enhancing the proton gradient with chlororespiration	38
4.3.4 Light-activated PGR5 efficiently protects PSI from further damage under high light	40
<b>5 Discussion</b>	<b>41</b>
5.1 Phosphorylation-dependent protein complex rearrangements in the PSII–LHCII–PSI–LHCI megacomplex at the grana margins	41
5.1.1 Phosphorylation status of LHCB2 determines the association of PSI in the megacomplex	42
5.1.2 STN7-dependent rearrangements over-ride any STN8-dependent changes in grana stacking	44
5.1.3 Similar light-intensity-dependent dynamics of PSI and Cyt $b_6f$ might protect PSI from photoinhibition	44
5.2 PGR5, NDH-1 and PTOX protect PSI from photoinhibition by modulating the proton gradient	46
5.2.1 PGR5 only modulates the rate of CET indirectly	46
5.2.2 PGR5 protects PSI from photoinhibition by controlling the electron flow from PSII to PSI under excess light	47

5.2.3 NDH-1 and PTOX mitigate PSI photoinhibition by generating a proton gradient under light-limiting conditions	50
<b>6 Conclusions</b>	<b>52</b>
<b>7 Future perspectives</b>	<b>53</b>
<b>Abbreviations</b>	<b>54</b>
<b>References</b>	<b>57</b>
<b>Paper I</b>	<b>65</b>
<b>Paper II</b>	<b>79</b>
<b>Paper III</b>	<b>93</b>
<b>Paper IV</b>	<b>101</b>

# 1 Introduction

Virtually all life on Earth is dependent on organic compounds that are built from atmospheric carbon dioxide (CO<sub>2</sub>) using energy from the sun in a process called photosynthesis. Although organic compounds are the end products of photosynthesis, the side product, molecular oxygen (O<sub>2</sub>) is equally important for major fraction of life. Photosynthetic organisms comprise anoxygenic photosynthetic bacteria, cyanobacteria, algae and land plants that include mosses, ferns, conifers and flowering plants. In algae and land plants, photosynthesis takes place in cell organelles called chloroplasts that are originally evolved from cyanobacteria. Photosynthesis is composed of two spatially separated processes: water-splitting light reactions and carbon reduction reactions. Protein complexes catalysing the photosynthetic light reactions are embedded in the thylakoid membrane, which is a lipid bilayer enclosing an aqueous space, lumen, that is separated from the surrounding chloroplast stroma. The light reactions bind the light energy into chemical forms – NADPH and ATP – which are then used in CO<sub>2</sub> fixation.

## 1.1 Photosynthetic light reactions

Photosynthetic light reactions are catalysed by pigment–protein complexes Photosystem (PS)II and PSI (Figure 1). The light energy for the process is harvested by specialized pigment-protein complexes called light-harvesting complexes (LHCs), in which the energy is transferred from one pigment to another mostly by resonance energy transfer (Förster, 1946; Förster, 1948) until it reaches the reaction centre of a photosystem. From the two types of LHCs, LHCI collects excitation energy only for PSI, while LHCII functions as a shared antenna for both photosystems (Wientjes et al., 2013a; Grieco et al., 2015). With the absorbed light energy, a specialized pair of chlorophyll *a* pigments in the photosystem reaction centre, denoted as P680 for PSII and P700 for PSI, gets excited and donates an electron to a specific primary electron acceptor. This primary charge separation creates a pair of oppositely charged radicals and, in fact, the entire electron transfer

## INTRODUCTION

chain (ETC) is based on the formation of a series of radical pairs, each of which is more stable than the previous one, which prevents the recombination of the charges.

The photosynthetic light reactions begin when P680 gets excited (P680\*) and donates an electron to pheophytin (Figure 1). In approximately 3 ps, the charges between P680\* and pheophytin are separated (Hughes et al., 2006) and in ~250 ps, pheophytin has reduced the plastoquinone (PQ) at the Q<sub>A</sub> site of the reaction centre protein D2 (Demeter and Govindjee, 1989; Govindjee et al., 2017). From Q<sub>A</sub>, the electron is subsequently transferred to another PQ molecule that resides in the Q<sub>B</sub> pocket of the reaction centre protein D1. After accepting two electrons and two protons, the PQ detaches from the Q<sub>B</sub> site into the thylakoid membrane as a fully reduced plastoquinone PQH<sub>2</sub> ( $\text{PQ} + 2 \text{e}^- + 2 \text{H}^+ \rightarrow \text{PQH}_2$ ), which is then replaced with an oxidized PQ (Demeter and Govindjee, 1989; Govindjee et al., 2017) (Figure 1). As an extremely strong oxidant, P680<sup>+</sup> receives a complementary electron from tyrosine Z (Y<sub>Z</sub>) of the reaction centre protein D1 in 20 ns–35 μs (Govindjee et al., 2017). Y<sub>Z</sub> derives this electron from the Mn<sub>4</sub>CaO<sub>5</sub> complex, which oxidizes the ultimate electron source, a water molecule (H<sub>2</sub>O), producing O<sub>2</sub> as side product ( $2 \text{H}_2\text{O} \rightarrow 2 \text{e}^- + 2 \text{H}^+ + \text{O}_2$ ).

The next complex in the ETC, Cytochrome (Cyt) b<sub>6</sub>f, oxidizes the PQH<sub>2</sub> bound to the Q<sub>0</sub> site of the complex. The step between PSII and Cyt b<sub>6</sub>f forms the main bottleneck in the entire ETC: altogether the exchange of PQH<sub>2</sub> to PQ at the Q<sub>B</sub> site, the diffusion of PQH<sub>2</sub> and the oxidation of it at the Q<sub>0</sub> site take approximately 5 ms (Demeter and Govindjee, 1989). At the Q<sub>0</sub> site, PQH<sub>2</sub> is oxidized ( $\text{PQH}_2 \rightarrow \text{PQ} + 2 \text{e}^- + 2 \text{H}^+$ ). The two protons of PQH<sub>2</sub> are released to the lumen, whereas from the two electrons, one reduces the Rieske iron-sulphur (FeS) centre and the other one reduces the so called low-potential heme b<sub>L</sub> of Cyt b<sub>6</sub> (Kallas, 2012; Dumas et al., 2016). Next, the first electron from the FeS centre reduces plastocyanin in the thylakoid lumen via Cyt f, while the other electron is transferred via the high-potential heme b<sub>H</sub> to the Q<sub>i</sub> site of the Cyt b<sub>6</sub>f complex where it reduces a free PQ. After receiving two electrons and two protons from the stroma, the PQ is released from the Q<sub>i</sub> site as fully reduced PQH<sub>2</sub> into the thylakoid membrane and oxidized again at the Q<sub>0</sub> site of the Cyt b<sub>6</sub>f complex. This so called Q cycle doubles the proton translocation from stroma to lumen.

When PSI gets excited, charges separate between P700\* and a special chlorophyll *a* designated as A<sub>0</sub> (Figure 1), but unlike in PSII, this charge separation only takes less than 1 ps (Demeter and Govindjee, 1989; Govindjee et al., 2017). The oxidized P700 (P700<sup>+</sup>) accepts a complementary electron from the water-soluble plastocyanin, and the charge separation is stabilized in ~20 ps when A<sub>0</sub> reduces a phylloquinone A<sub>1</sub> and when, in ~100 ns, A<sub>1</sub> donates the electron to an iron-sulphur (FeS) cluster series: F<sub>X</sub>, F<sub>A</sub> and F<sub>B</sub> (Demeter and Govindjee, 1989; Govindjee et al., 2017). Electrons from the FeS clusters reduce ferredoxin and, finally, ferredoxin-

## INTRODUCTION

NADPH-oxidoreductase (FNR) uses the electrons to reduce  $\text{NADP}^+$  to NADPH ( $\text{NADP}^+ + 2 e^- + \text{H}^+ \rightarrow \text{NADPH}$ ). Additionally, the electrons from ferredoxin can be cycled back to the PQ pool by NDH-1 (Figure 1), which is discussed in more detail in section 1.6.4.

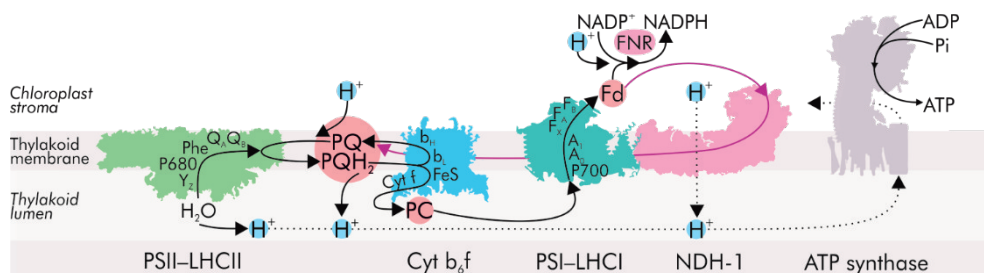


**Figure 1. The protein complexes and electron transfer chain of photosynthetic light reactions.** During the light reactions, electrons are transferred from  $\text{H}_2\text{O}$  to  $\text{NADP}^+$  by thylakoid protein complexes Photosystem (PS)II, Cytochrome (Cyt)  $b_6/f$  and PSI as well as by mobile electron carriers plastoquinone (PQ), plastocyanin (PC) and ferredoxin (Fd). The light reactions begin when the special chlorophyll pair of PSII, P680, gets excited and donates an electron to pheophytin (Phe). Phe transfers the electron to a PQ at the  $Q_A$  site, from where the electron reduces another PQ at the  $Q_B$  site. After accepting two electrons and two protons, the PQ at  $Q_B$  site detaches as  $\text{PQH}_2$  and is replaced by another PQ. The electron donated by P680 is replaced by  $Y_z$ , which drains electrons from the water oxidizing complex of PSII. The mobile  $\text{PQH}_2$  is oxidized by Cyt  $b_6/f$ , and one electron reduces the Rieske FeS centre and the other the  $b_L$  heme. The electron from the FeS centre reduces PC via Cyt f, while the electron from  $b_L$  reduces another PQ via  $b_H$  heme. The PC is oxidized at PSI by the excited P700, which starts an electron transfer chain to Fd via chlorophyll  $A_0$ , phylloquinone  $A_1$  and the FeS centres  $F_x$ ,  $F_A$  and  $F_B$ . Finally, FNR uses the electron from  $\text{H}_2\text{O}$  to reduce  $\text{NADP}^+$  into NADPH. In addition to the above-described linear electron transfer, NDH-1 can cycle the electrons from Fd back into the PQ pool (purple arrow). The oxidation of  $\text{H}_2\text{O}$  by PSII releases protons in the thylakoid lumen and the electron transfer through Cyt  $b_6/f$  and NDH-1 is coupled with proton translocation from the chloroplast stroma into the thylakoid lumen and as a consequence, an electrochemical gradient is formed across the thylakoid membrane. The gradient drives the synthesis of ATP by the ATP synthase. Together the end products of the light reactions, NADPH and ATP, are used to bind atmospheric  $\text{CO}_2$  into sugar compounds. The crystal structures and Cryo-EM density maps used for the figure were obtained from Su et al., 2017 (PSII-LHCII), Stroebel et al., 2003 (Cyt  $b_6/f$ ), Ben-Shem et al., 2003 (PSI-LHCI), Laughlin et al., 2019 (NDH-1) and Abrahams et al., 1994 (ATP synthase).

During the ETC, an electrochemical gradient is formed across the thylakoid membrane. This results from the fact that, per two electrons, the oxidation of water at PSII releases two protons into the thylakoid lumen, together the reduction of PQ and oxidation of  $\text{PQH}_2$  translocate three protons from the chloroplast stroma into the thylakoid lumen, while the reduction of  $\text{NADP}^+$  consumes one proton from the chloroplast stroma. The consequent acidification of the lumen is linked to important regulatory mechanisms discussed in section 1.6. Moreover, the electrochemical gradient acts as a proton motive force that drives ATP synthase, which releases protons from the lumen to the stroma and couples the proton pumping to the synthesis of ATP (Mitchell, 1966). It has been estimated that, per one electron, maximally 0.64 ATP molecules can be produced (Foyer et al., 2012). Together, the

## INTRODUCTION

NADPH and ATP produced in the photosynthetic light reactions are used to capture and reduce atmospheric carbon dioxide into organic compounds.

### 1.2 Structure and interactions of the photosystems

PSII functions as a dimer. Depending on the species, each monomer contains 20–23 protein subunits and can be divided into a core and an oxygen-evolving complex (Umena et al., 2011; Wei et al., 2016; Bezouwen et al., 2017). In terms of the core proteins, PSBA (D1) and PSBD (D2) bind all the cofactors required in ETC at PSII, whereas PSBB (CP47) and PSBC (CP43) function in light harvesting. The oxygen-evolving complex includes a species-specific set of protective protein subunits and the actual  $Mn_4CaO_5$  cluster catalysing the oxidation of water (Bezouwen et al., 2017). In addition to the monomeric internal antenna proteins CP47 and CP43, excitation energy is collected by LHCII trimers, which are bound to the PSII dimer in variable amounts. The LHCII trimers, in turn, are composed of LHCB1–3 proteins (Jansson, 1994) and bound to PSII via monomeric antenna proteins LHCB4–6 (Boekema et al., 1999; Kouřil et al., 2012). Depending on their strength of association with PSII, the LHCII complexes can be designated as either strongly (S), moderately (M) or loosely (L) bound LHCII. The S-LHCII consists of the LHCB1 and LHCB2 proteins and is strongly attached to PSII via the LHCB5 protein, whereas the M-LHCII is composed of LHCB1 and LHCB3 and is bound to PSII via the LHCB4 and LHCB6 proteins (Boekema et al., 1998; Kouřil et al., 2012). L-LHCII contains LHCB1, LHCB2 and LHCB3 proteins, but the details of its attachment to PSII are still unclear (Boekema et al., 1999; Kouřil et al., 2012).

Eukaryotic PSI functions as a monomer containing 16 protein subunits of which PSAA and PSAB bind the catalytic cofactors participating in ETC at PSI (Caspary and Nelson, 2018). In addition to conserved core antenna, the plant PSI binds four additional pigment-proteins LHCA1–4 proteins, which form a stable LHCI antenna (Ben-Shem et al., 2003). The PSI–LHCI complex can occasionally interact with the NDH-1 complex via two other LHCI proteins, LHCA5 and LHCA6 (Peng et al., 2009). In addition to LHCI, excitation energy for PSI is collected by L-LHCII (Wientjes et al., 2013a; Grieco et al., 2015; Akhtar et al., 2016; Bos et al., 2017; Rantala et al., 2017) that can bind on the LHCI antenna (Benson et al., 2015) or directly on PSI via the PSAH protein (Lunde et al., 2000).

### 1.3 Thylakoid structure and dynamics

The thylakoid, according to its name in Greek, “thylakos”, meaning “a sac”, is a continuous membrane structure that, in higher plants, is mostly folded into so-called grana stacks that are connected by one-layered thylakoid structures known as stroma



## INTRODUCTION

thylakoids (Figure 2). The stroma thylakoids appear to wind around the grana stacks at an angle of 20–25° (Paolillo, 1970; Mustárdy and Garab, 2003; Mustárdy et al., 2008; Austin and Staehelin, 2011; Daum and Kühlbrandt, 2011). Most of the thylakoid area comprises protein complexes that are heterogeneously distributed between the grana stacks and the stroma thylakoids. The location of the protein complexes of the ETC is based on the height of their stromal projections as well as the size of the stromal gap between the layers of the grana stacks. As depicted in Figure 2, the relatively flat-structured PSII–LHCII complexes are enriched in the appressed grana stacks, whereas PSI–LHCI, NDH-1 and ATP synthase are unable to enter between the layers due to their long stromal protrusions and, as a result, reside on the non-appressed stroma thylakoids instead (Miller and Staehelin, 1976; Andersson and Anderson, 1980; Sirpiö et al., 2009). However, no consensus exists about the exact location of Cyt *b*<sub>6</sub>*f*, but because the width of the stromal gap varies between 3.2 and 4.2 nm, depending on light conditions, the complex is thought to enter the grana stacks at least occasionally (Kirchhoff et al., 2017).

In addition to the grana and stroma thylakoids, a third thylakoid region – grana margins – has been recognized. It contradicts the concept of strict lateral heterogeneity by harbouring both photosystems (Albertsson, 2001; Danielsson and Albertsson, 2009; Järvi et al., 2011; Suorsa et al., 2014) and by enabling dynamic interaction and energy transfer between PSII–LHCII and PSI–LHCI (Suorsa et al., 2015; Yokono et al., 2015; Yokono and Akimoto, 2018). Originally this specific region was thought to consist of a ring-like structure on the grana periphery i.e. margins (Albertsson, 2001). However, the highly curved regions now have been demonstrated to be incapable of harbouring any membrane protein complexes and, for this reason, they likely only contain proteins directly needed for the membrane folding (Murphy, 1986; Dekker and Boekema, 2005; Kouřil et al., 2011; Armbruster et al., 2013). Instead of the actual periphery of the grana stacks, the grana margins seem to comprise a distinct membrane region between the appressed grana stacks and the non-appressed stroma thylakoids (Figure 2), and such model for grana margins is also used throughout this book. Whether the nature of this interphase is a tubular membrane branch or a simple continuum from the surrounding stroma thylakoids, remains to be solved (Paolillo, 1970; Mustárdy et al., 2008; Austin and Staehelin, 2011; Daum and Kühlbrandt, 2011).

As the distribution of protein complexes relies on the folding of the membrane, so does the grana stacking depend on the protein complexes. The major force attaching neighbouring grana layers to each other is thought to compose of cation screening between the negatively charged amino acids of adjacent LHCII complexes (Barber, 1980). The attraction between the positively and negatively charged amino acids of LHCII (Standfuss et al., 2005) as well as various interactions between protein complexes and lipids also play a role (Dekker and Boekema, 2005). Since

## INTRODUCTION

thylakoid folding is based on relatively weak interactions, it is easily affected by the alterations in the chemical environment that reflect the state of photosynthetic light reactions. When plants are exposed to light after a period of darkness, the intensified proton gradient accumulates  $\text{Cl}^-$  (Spetea and Schoefs, 2010) and  $\text{Ca}^{2+}$  ions in the thylakoid lumen (Ettinger et al., 1999) and as an osmotic result, the lumen swells (Kirchhoff et al., 2011). As a response to changing light conditions, the thylakoid membrane is capable of reoptimizing its stacking within minutes (Rozak et al., 2002). Compared to darkness, chloroplasts in low light conditions show narrower (Kyle et al., 1983) but more grana stacks with increased number of layers (Kyle et al., 1983; Anderson, 1986; Rozak et al., 2002; Wood et al., 2019). High light intensity, on the other hand, seem to result in fewer but wider grana stacks with less layers (Anderson, 1986; Rozak et al., 2002; Fristedt et al., 2009; Wood et al., 2019).

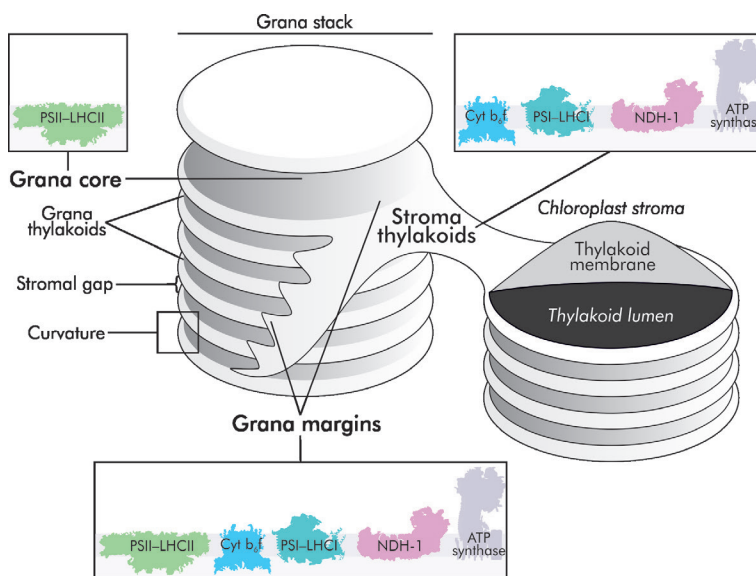


**Figure 2. Thylakoid structure and composition.** The thylakoid membrane of a plant chloroplast is partly appressed into grana stacks, and the layers of the stacks are called grana thylakoids. The area between the layers is designated as the grana core and the peripheral area as curvature. The separate grana stacks are connected by non-appressed stroma thylakoids, and the distal regions of the appressed grana stacks, continuing as non-appressed stroma thylakoids, are designated as grana margins. The thylakoid system encloses a continuous aqueous phase, lumen. The protein complexes are heterogeneously distributed in the thylakoid membrane: PSII-LHCII is found on the appressed membranes, while the larger PSI-LHCI, NDH-1 and ATP synthase are located on the non-appressed membranes. The location of Cyt b<sub>6</sub>f is likely dynamically regulated based on the size of the stromal gap. The protein complexes are able to meet at the grana margins.

## 1.4 Thylakoid fractionation

Decades of research has provided a robust view of the thylakoid system, but the details – especially on the nature of the grana margins – are still elusive. In the absence of a direct way of visualizing protein complexes attached to the membrane, the function of the thylakoid system has been extensively studied by fractionating it into its structural compartments, either mechanically or chemically.

Mechanical fractionation makes use of sonication or press treatment to separate the grana core, grana margins and stroma lamellae (Andreasson et al., 1988). The grana cores obtained with mechanical fractionation are enriched in PSII–LHCII, the margins with both PSII–LHCII and PSI and stroma vesicles with PSI and ATP synthase (Suorsa et al., 2014). In addition to the grana core, margins and stroma lamellae, the press treatment of isolated thylakoid membranes results in the so-called Y-100 fraction, which is highly enriched in PSI and ATP synthase and is thus thought to represent either very pure stroma lamellae or the end membranes of the grana stacks (Jansson et al., 1997; Danielsson et al., 2004; Danielsson and Albertsson, 2009; Suorsa et al., 2014). Dimeric Cyt  $b_6/f$  is found in all of the fractions obtained with mechanical fractionation (Danielsson and Albertsson, 2009), yet details on its preferential location are missing.

Chemical fractionation relies on weak non-ionic detergents. The detergents solubilize protein complexes at their characteristic capacity, thus resulting in different-sized lipid-protein assemblies that are collected by centrifugation. For over 50 years, 0.2–2 % digitonin has been used to divide the thylakoid system into the appressed and non-appressed membranes (Boardman and Anderson, 1964; Anderson and Boardman, 1966; Kyle et al., 1984; Baena-González et al., 1999). The capacity of digitonin to separate the two thylakoid fractions is based on its size. As a large molecule, digitonin is unable to reach the appressed grana core with tightly packed protein complexes, but it easily releases the relatively small complexes from the non-appressed stroma thylakoids, end membranes and grana margins (Järvi et al., 2011). This differential solubilization results in thylakoid membrane fractions with distinct protein complex composition that consequently form pellets at different g forces (Anderson and Boardman, 1966).

Prior to the separation of the digitonin-solubilized thylakoid fractions, the insoluble material is removed with centrifugation at  $1,000\text{--}4,500 \times g$  (Anderson and Boardman, 1966; Kyle et al., 1984; Baena-González et al., 1999). The resulting fractions are then always pelleted from the remaining supernatant. According to the first-described fractionation method, the grana cores are collected at  $10,000 \times g$ , the interphase at  $40,000\text{--}50,000 \times g$  and, finally, the stroma thylakoids at  $144,000 \times g$  (Anderson and Boardman, 1966; Kyle et al., 1984). The  $10,000 \times g$  and  $144,000 \times g$  fractions have been confirmed to represent the grana core and stroma thylakoids due to their enrichment in PSII and PSI, respectively (Kyle et al., 1984). The interphase

## INTRODUCTION

obtained with  $40\,000\text{--}50,000 \times g$ , however, is more problematic: some believe it only contains grana margins (Georgakopoulos and Argyroudi-Akoyunoglou, 1994), while for others, it represents the whole grana, from which the grana core and grana margins can be separated with another weak detergent, Triton X-100, and re-centrifugation at  $40,000 \times g$  (Baena-González et al., 1999). Furthermore, the digitonin-insoluble grana core can be opened with dodecyl maltoside, which is able to solubilize the whole thylakoid system since it can also enter the grana stacks (Järvi et al., 2011).

### 1.5 Photoinhibition of the photosystems

In addition to its essential role in harvesting and transducing solar energy, photosynthesis is a central regulator between light energy input and metabolic requirements. Too little light stunts growth and development, but too much light also has severe consequences. If excess light is channelled to the PSII reaction centre, it causes oxidative damage. Even though photoinhibition is directly proportional to light intensity (Tyystjärvi and Aro, 1996), it is important to note that also low light can be excessive if it is insufficiently controlled i.e. used either for photochemistry or dissipated as heat (Demmig-Adams and Adams, 1992).

No consensus exists on the exact reason leading to PSII photoinhibition, but the damage is known to be oxidative and focused on the PSII reaction centre protein D1, which undergoes a continuous repair cycle (Aro et al., 1993; Järvi et al., 2015). First, the damaged and phosphorylated PSII is monomerized and transferred to the non-appressed membranes (Aro et al., 2005) which also house the proteases and auxiliary proteins (Suorsa et al., 2014). Next, the monomeric PSII is dephosphorylated and disassembled, after which the proteases are able to degrade the damaged D1 (Rintamäki et al., 1996). Novel D1 is then co-translationally synthesized into the PSII subcomplex (Zhang et al., 1999), and the fully assembled complex monomer returns to the grana core to dimerize and interact with LHCI (Rokka et al., 2005). Since the repair cycle involves the migration of the damaged PSII from the grana stacks to the non-appressed membranes, the high-light-induced partial de-stacking and lateral shrinking of the grana stacks are thought to facilitate the repair cycle (Tikkanen et al., 2008; Fristedt et al., 2009).

While PSII is extremely vulnerable to excess excitation energy, PSI has poor tolerance for excess electrons. Photoinhibition of PSI has been observed under conditions saturating the PSI electron acceptors, such as under low temperature (Terashima et al., 1994; Zhang and Scheller, 2004) and under fluctuating light (Suorsa et al., 2012). It has been recently reported to drastically affect the primary metabolism, such as carbon fixation and starch accumulation (Gollan et al., 2017; Lima-Melo et al., 2018). In the absence of free electron acceptors, the electrons

## INTRODUCTION

accumulated in the FeS centres of PSI are donated to O<sub>2</sub> instead, resulting in the formation of superoxide anion (O<sub>2</sub><sup>-</sup>), which is rapidly turned into hydrogen peroxide (H<sub>2</sub>O<sub>2</sub>) by superoxide dismutase (Asada, 1999). A reaction between H<sub>2</sub>O<sub>2</sub> and the reduced acceptor side of PSI, on the other hand, produces hydroxide anion (OH<sup>-</sup>), which destroys the iron-sulphur centres (Sonoike et al., 1997). To prevent this harmful reaction, ascorbate peroxidase catalyses the scavenging of H<sub>2</sub>O<sub>2</sub> into H<sub>2</sub>O (Asada, 1999). In addition, the limitations in electron transfer favours the electron spin of P700\* to transition from singlet to triplet state (<sup>3</sup>P700), which, when reacting with O<sub>2</sub>, produces extremely harmful singlet oxygen (<sup>1</sup>O<sub>2</sub>) (Shuvalov et al., 1986; Cazzaniga et al., 2012). No efficient repair cycle exists for the inhibited PSI and, for this reason, the rapid damage at the FeS centres is followed by the extremely slow degradation of both reaction centre proteins, PSAA and PSAB. In addition, several other smaller chlorophyll-binding subunits on the acceptor side are degraded due to their retained ability to absorb light and produce ROS (Tjus et al., 1999; Kudoh and Sonoike, 2002). In fact, it has been demonstrated that the pigment-rich LHCI antenna is released and degraded as the first emergency measure (Alboresi et al., 2009; Krumova et al., 2014).

### 1.6 Regulation of light reactions

Constantly changing light conditions challenge plants to balance between efficient photosynthesis and avoiding photodamage. As sessile organisms, plants are unable to relocate themselves to a more suitable environment but, instead, optimize the amount of light by redirecting their leaves, reorganizing their chloroplasts as well as adjusting their photosystem and antenna stoichiometry and chlorophyll content. In addition to these strategies, fine-tuning the photosynthetic light reactions is necessary especially in order to avoid excess electrons accumulating and damaging PSI, which lacks an efficient repair cycle. For this reason, plants have developed a variety of molecular regulatory mechanisms controlling both excitation energy harvesting (sections 1.6.1 and 1.6.2) and electron transfer (sections 1.6.3, 1.6.4 and 1.6.5) in order to prevent the accumulation of excess electrons at PSI.

#### 1.6.1 Phosphorylation of LHCII and PSII core proteins

Under low light intensities, the binding of PQH<sub>2</sub> to the Q<sub>0</sub> site of Cyt b<sub>6</sub>f activates the STATE TRANSITION7 (STN7) kinase (Vener et al., 1997; Rintamäki et al., 2000) in a process involving reversible autophosphorylation (Willig et al., 2011; Trotta et al., 2016). Active STN7 phosphorylates LHCII subunits LHCB1 and LHCB2 (Depège et al., 2003; Bellafiore et al., 2005; Bonardi et al., 2005), which increases the affinity of LHCII towards PSI (Lunde et al., 2000; Bellafiore et al.,

## INTRODUCTION

2005). The phosphorylation of LHCII is maximal at light intensities lower than the prevailing growth conditions (Rintamäki et al., 1997; Rintamäki et al., 2000). An increase in light intensity accelerates PQH<sub>2</sub> binding but also results in the reduction of stromal thioredoxins that inactivate STN7 (Rintamäki et al., 2000). The inactivation of STN7 enables the dephosphorylation of LHCII by THYLAKOID-ASSOCIATED PHOSPHATASE of 38 kDa / PROTEIN PHOSPHATASE1 (TAP38/PPH1) (Pribil et al., 2010; Shapiguzov et al., 2010), which has recently been reported to associate with the PSII–LHCII–PSI–LHCI megacomplex (Rantala et al., 2016).

The reversible phosphorylation of LHCII in plants has been traditionally related to the so-called state transition model (Bennett et al., 1980; Allen et al., 1981; Horton and Black, 1981). According to the model, a part of the LHCII migrates between the photosystems during an excitation imbalance. In the case of over-excitation of PSII, LHCII is thought to detach from PSII in the grana core and to travel to the stroma thylakoids to collect excitation energy for PSI instead (state 2), and, vice versa, if PSI gets over-excited, LHCII returns to the grana core (state 1). In a laboratory, such state transitions are induced using certain light qualities: state 2 with red light and state 1 with far-red light. In view of recent literature, the state transition model has, however, been questioned. First of all, the dense protein complex packing likely hampers the movement of LHCII between the appressed and nonappressed membranes (Kirchhoff et al., 2008). Secondly, the model requires a strict lateral heterogeneity of PSII and PSI, while the recent data points towards an interaction between the two photosystems in the grana margins (Suorsa et al., 2015; Rantala et al., 2017). Thirdly, a certain fraction of LHCII complexes is phosphorylated in all light conditions and in all compartments of the thylakoids (Tikkanen et al., 2008; Grieco et al., 2012). Finally, only phosphorylated L-LHCII, representing a small fraction of all LHCII complexes, is capable of associating with PSI, (Rantala et al., 2017), while the S- and M-LHCII in grana core stay confined to PSII even when phosphorylated (Wientjes et al., 2013b).

In addition to LHCB1 and LHCB2, at low light conditions the STN7 kinase is partially involved in phosphorylation of the PSII core proteins D1, D2 and CP43, as well as the monomeric antenna protein LCHB4 (Bellafiore et al., 2005; Bonardi et al., 2005; Tikkanen et al., 2006). More specifically, though, the PSII core protein phosphorylation is regulated by the STATE TRANSITION8 kinase (STN8) and the PHOTOSYSTEM II CORE PHOSPHATASE, which both target the PSII reaction centre proteins D1, D2 and CP43 (Bonardi et al., 2005; Vainonen et al., 2005; Samol et al., 2012). The activation and inactivation methods of these enzymes are unknown, but the phosphorylation of the PSII core is the most prominent in high light (Rintamäki et al., 1997), under which it is thought to enable the rearrangement of the

## INTRODUCTION

PSII–LHCII supercomplexes in the grana core, thus to facilitating the D1 repair cycle (Tikkanen et al., 2008; Fristedt et al., 2009; Goral et al., 2010).

### 1.6.2 Thermal dissipation of excess excitation energy from LHCII

When light intensity increases, protons accumulate in the lumen and activate the thermal dissipation of excess excitation energy from the LHCII antenna in a process involving the re-organization of LHCII complexes (Horton et al., 1991; Horton et al., 2005; Betterle et al., 2009; Holzwarth et al., 2009; Correa-Galvis et al., 2016). The dissipation process is known to be triggered through the de-epoxidation of violaxanthin to zeaxanthin (xanthophyll cycle) (Demmig-Adams, 1990) and/or the protonation of the luminal glutamate residues 122 and 226 of a membrane-intrinsic LHC protein family member, the PSBS protein (Li et al., 2000; Li et al., 2004). PSBS associates with the PSII core as a dimer, whereas protonation monomerizes the protein (Bergantino et al., 2003) and enhances its interaction with LHCB1 of M-LHCII (Correa-Galvis et al., 2016). PSBS seems to enable the re-organization of PSII–LHCII complexes into a dissipative state by enhancing their fluidity (Kiss et al., 2008; Goral et al., 2012). This mode of LHCII has been suggested to be an LHCII aggregate (Horton et al., 1991; Horton et al., 2005), a dissociated LHCII trimer (Holzwarth et al., 2009) or a disintegrated pentamer LHCII–CP24–CP29 (Betterle et al., 2009).

### 1.6.3 Photosynthetic control of electron transfer through Cyt $b_6f$ complex

In addition to thermal dissipation, acidification of the lumen induces the so-called photosynthetic control of electron transfer, which is based on the pH sensitivity of PQH<sub>2</sub> oxidation at Cyt  $b_6f$  (Rumberg and Siggel, 1969; Stiehl and Witt, 1969). The first step in the oxidation process is a formation of a hydrogen bond between PQH<sub>2</sub> and a histidine residue in the vicinity of the Rieske FeS centre at the Q<sub>0</sub> site of Cyt  $b_6f$  (Crofts et al., 1999), and thus, protonation of the histidine residue prevents the binding of PQH<sub>2</sub>. Consequently, ETC automatically slows down if the electrons entering the chain from PSII exceed the capacity of the PSI electron acceptors – e.g. when light intensity becomes excess or the carbon binding reactions begin to limit the flow of electrons in the ETC. Thus, photosynthetic control efficiently prevents PSI from photoinhibition by eliminating the over-reduction of PSI acceptor side (Joliot and Johnson, 2011; Suorsa et al., 2012).

### 1.6.4 NDH-1-dependent electron transfer

Another way to protect PSI from saturation and damage is to redirect electrons from ferredoxin back to the PQ pool instead of FNR (Figure 1). This cyclic electron

## INTRODUCTION

transfer (CET) strengthens the proton gradient and consequently enhances photosynthetic control, thermal dissipation and synthesis of ATP. It has been suggested that the division of electrons between LET and CET could be determined by the redox state of PSI donors and acceptors (Breyton et al., 2006). Consensus exists that CET is mediated by an NAD(P)H PQ oxidoreductase called type I NADH dehydrogenase (NDH-1) (Burrows et al., 1998; Rumeau et al., 2005; Yamamoto et al., 2011). Due to its large stromal protrusions, NDH-1 is located in the non-appressed membranes (Lennon et al., 2003) where it has been reported to physically interact with 1 % of PSI (Peng et al., 2009; Järvi et al., 2011). Per one electron, NDH-1 is able to transfer four protons from the stroma to the lumen: two via the Q cycle and two via direct pumping (Strand et al., 2017). NDH-1-dependent CET has been shown to function on the onset of illumination and under low light (Yamori et al., 2015). In addition to CET, NDH-1 is known to mediate chlororespiration with PLASTID TERMINAL OXIDASE (PTOX), a small thylakoid protein (Carol et al., 1999; Wu et al., 1999; Cournac et al., 2000; Rumeau et al., 2007). During chlororespiration, NDH-1 feeds the PQ pool with electrons that PTOX uses to reduce O<sub>2</sub> to H<sub>2</sub>O (Bennoun, 1982; Cournac et al., 2000; Rumeau et al., 2007).

### 1.6.5 PGR5-dependent control of electron transfer

CET was first discovered in the form of oxygen-independent production of ATP coupled with carbon fixation (Arnon et al., 1954). This so-called cyclic phosphorylation was then found to require ferredoxin and to be sensitive to antimycin A (Tagawa et al., 1963). Since NDH-1-dependent CET was concluded to be insensitive to antimycin A (Endo et al., 1997), the antimycin A-sensitive CET pathway was suggested to rely on the PROTON GRADIENT REGULATIONS5 (PGR5) protein (Munekage et al., 2002) or its membrane anchor PROTON GRADIENT REGULATION LIKE1 (PGRL1) (Munekage et al., 2002; DalCorso et al., 2008; Hertle et al., 2013). PGR5 has been demonstrated to be enriched in both the grana core and stroma thylakoids, whereas PGRL1 is mostly found only on the stroma thylakoids (Suorsa et al., 2014). As thermal dissipation is affected in the absence of PGR5, it has been suggested that the protein mediates CET that specifically down-regulates PSII by inducing thermal dissipation at LHCII (Munekage et al., 2002). Since its discovery, however, a considerable amount of evidence has accumulated that contradicts the previously assumed role of PGR5 in CET, and, for this reason, a hypothesis on PGR5 as a modulator of LET has emerged (see Discussion).



## 2 Aims of the Study

The goal of this thesis project was to elucidate the functional relationship between the molecular regulatory mechanisms that are induced by increased light intensity in order to keep ETC optimally oxidized to protect PSI. The specific aims were:

- i to examine the energetic connectivity between PSII–LHCII and PSI–LHCI at the grana margins by analyzing the appressed and non-appressed thylakoid membranes with detergents (Paper I),
- ii to determine the role of the reversible phosphorylation of PSII and LHCII proteins in the thylakoid protein complex rearrangements upon increase in light intensity by gradually fractionating the non-appressed thylakoid membranes with digitonin (Paper I),
- iii to discover specific fluorescence and P700 parameters reflecting the activity of reversible phosphorylation, thermal dissipation and photosynthetic control that keep ETC optimally oxidized (Paper II),
- iv to elucidate the role of PGR5 in modulating photosynthetic electron transfer (Papers II and III) and
- v to investigate the possible roles of PGR5 and NDH-1 in the acclimation of the photosynthetic light reactions to PSI photoinhibition (Paper IV).

## 3 Methodology

### 3.1 Plant lines and their growth and treatments

To assess the specific function of the regulatory proteins, knock-out mutants lacking the functional genes that encode these proteins were compared to *Arabidopsis thaliana* wild-type Columbia (WT). The transgenic lines along with their description and reference as well as paper(s) of this thesis studying the lines are presented in Table 1. The plants were grown at 23 °C and 60 % relative humidity under an 8-hour photoperiod of either low, moderate or high light (50, 120 or 500  $\mu\text{mol photons m}^{-2} \text{s}^{-1}$ , respectively) with POWERSTAR HQI-T 400 W/D metal halide lamps (OSRAM GmbH, Munich, Germany) as the light source. Prior to experiments, some plants were treated with 2 h of high light (600  $\mu\text{mol photons m}^{-2} \text{s}^{-1}$ ) (Paper I), some with 3 days of fluctuating light (50  $\mu\text{mol photons m}^{-2} \text{s}^{-1}$  for 5 min and 500  $\mu\text{mol photons m}^{-2} \text{s}^{-1}$  for 1 min under an 8-hour photoperiod) (Paper II) and some with 2 and 4 h of a PSI-inhibiting light regime, as explained in detail in Table 2 in Paper IV.

**Table 1. Transgenic lines of *Arabidopsis thaliana* used in this thesis.**

<b>Genotype and missing protein(s)</b>	<b>Molecular phenotype</b>	<b>Studied in Paper</b>
<i>pgr5</i> PGR5	Impaired proton gradient and thermal dissipation, reduced ETC (Munekage et al., 2002); depletion in PSI, upregulated ATP synthase and PTOX under fluctuating light (Suorsa et al., 2012)	II, III, IV
<i>ndho</i> NDHO	Lacking chloroplast NDH-1 complex (Rumeau et al., 2005)	IV
<i>npq4</i> PSBS	Impaired thermal dissipation seen as low non-photochemical quenching of fluorescence (Li et al., 2000)	II, III
<i>stn7</i> STN7	Absent phosphorylation of LHCB1 and LHCB2, decreased excitation and increased amount of PSI (Bellafiore et al., 2005)	I, II
<i>stn8</i> STN8	Decreased phosphorylation of CP43, D1 and D2 (Bonardi et al., 2005); increased membrane folding (Fristedt et al., 2009)	I
<i>stn7stn8</i> STN7 and STN8	Missing phosphorylation of LHCII and PSII (Bonardi et al., 2005); increased membrane folding (Fristedt et al., 2009)	I
<i>npq4stn7</i> PSBS and STN7	Absent LHCII phosphorylation and thermal dissipation (Frenkel et al., 2007)	II
<i>tap38/pph1</i> TAP38/PPH1	Missing dephosphorylation of LHCII under high light (Pribil et al., 2010; Shapiguzov et al., 2010)	I, II

### 3.2 Thylakoid isolation

In Papers I and IV, thylakoids from the leaves of 5 to 6-week-old plants were isolated one hour after the beginning of the daily photoperiod or after a specific light treatment, as explained in section 3.1. First, the rosettes were ground in grinding buffer (50 mM Hepes-NaOH pH 7.5, 330 mM sorbitol, 5 mM MgCl<sub>2</sub>, 0.05 % (w/v) BSA and 10 mM NaF) and filtered through Miracloth. Chloroplasts were collected by centrifugation at 3,952 × g for 7 min at 4 °C and ruptured osmotically in shock buffer (50 mM Hepes-NaOH pH 7.5, 5 mM sorbitol, 10 mM MgCl<sub>2</sub> and 10 mM NaF). The released thylakoids were collected by centrifugation at 3,952 × g for 7 min at 4 °C and suspended in storage buffer (50 mM Hepes-NaOH pH 7.5, 100 mM sorbitol, 10 mM MgCl<sub>2</sub>, and 10 mM NaF). Chlorophyll *a* and *b* concentration was determined according to Porra et al., 1989.

### 3.3 Gradual fractionation of thylakoids with digitonin

For gradual fractionation into its compartments in Paper I, the isolated thylakoids were diluted into storage buffer and solubilized with either 0, 0.25, 0.5, 1 or 2 % (w/v) digitonin (Calbiochem) and subjected to vigorous shaking for 8 min (Figure 3A). Due to its bulky nature, digitonin is only able to solubilize the non-appressed membranes. The non-appressed stroma thylakoids and grana margins were separated from the grana core by centrifugation at 18,620 × g for 25 min at 4 °C, after which the volume of both fractions was adjusted with storage buffer. The increasing concentration of digitonin was assumed to approach the non-appressed membranes gradually: the lowest concentration of digitonin was hypothesized to only break weak interactions in the stroma thylakoids, while the higher concentrations were expected to be able to dissect the PSII–LHCII–PSI–LHCI megacomplex in the grana margins (Figure 3B).

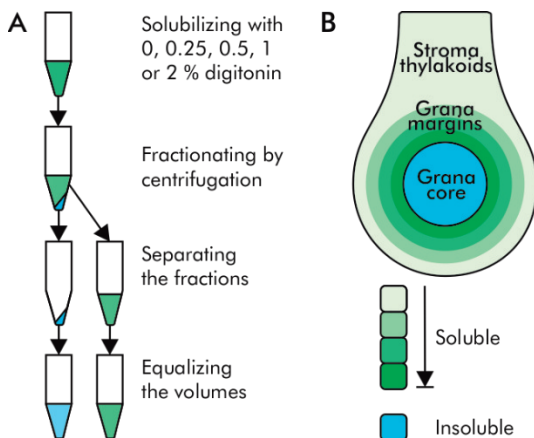


**Figure 3. Gradual digitonin solubilization.** **A.** Isolated thylakoids were solubilized with 0, 0.25, 0.5, 1 and 2 % of digitonin, after which the soluble fraction (green) was separated from the insoluble fraction (blue) with centrifugation and the volumes were equalized. **B.** A hypothetical model of the gradual dissection of the non-appressed membranes (green) by digitonin. The figure is modified from Figure 4 in Paper I.

### 3.4 Quantitating proteins with Western blotting

To compare the amount of certain proteins between the genotypes in Papers III and IV, isolated thylakoids were subjected to Western blotting. First, the membranes were solubilized with sample buffer (138 mM Tris-HCl pH 6.8, 6 M urea, 22.2 % (v/v) glycerol, 4.3 % (w/v) SDS, 10 % (v/v)  $\beta$ -mercaptoethanol), after which the insoluble material was removed by centrifugation at  $3,952 \times g$  for 5 min at room temperature. The solubilized proteins were then separated with SDS polyacrylamide gel electrophoresis (SDS-PAGE) with 15 % acrylamide and 6 M urea and subsequently transferred onto PVDF membrane (Millipore). Proteins of interest were recognized with specific antibodies and detected with horseradish peroxidase-linked secondary antibody (Agrisera) and Amersham ECL Western blotting detection reagents (GE Healthcare). To ensure equal sample content, all proteins were visualized with 0.1 % Coomassie Brilliant Blue diluted into 40 % (v/v) methanol and 10 % (v/v) acetic acid. Intensity of the antibody signal was quantified using GeneTools software (Syngene).

### 3.5 Visualizing protein complexes with blue native gel electrophoresis

For the protein complex analysis in Paper I, the thylakoids were fractionated with 1 % (w/v) digitonin as described in 3.3, but instead of storage buffer, the digitonin-soluble and -insoluble fractions were resuspended into a chlorophyll concentration of  $0.5 \mu\text{g}/\mu\text{l}$  with 25BTH20G buffer (25 mM Bis-Tris/HCl pH 7.0, 20 % (w/v) glycerol, and 0.25 mg/ml Pefabloc) (Järvi et al., 2011). The fractions were then further solubilized for 5 min on ice with 1 % (w/v) *n*-dodecyl  $\beta$ -D-maltoside (DM) (Sigma-Aldrich), which is capable of solubilizing almost all of the thylakoid system (Wittig et al., 2006). In addition to the double-solubilized samples, thylakoids solubilized with only 1 % (w/v) digitonin or DM were prepared. To add a negative charge, to avoid protein complex aggregation and to visualize pigmentless protein complexes, Serva Blue G buffer (100 mM Bis-Tris/HCl pH 7.0, 0.5 M ACA, 30 % (w/v) sucrose, and 50 mg/ml Serva Blue G) was added to a final concentration of 10 % (v/v). The protein complexes of the final samples ( $2 \mu\text{g}$  chlorophyll/ $\mu\text{l}$ ) were separated with large pore blue native gel electrophoresis (BN-PAGE) with an acrylamide gradient of 3–12.5 % (Järvi et al., 2011).

### 3.6 Measuring functional photosystems with fluorescence and absorption signal

As described in section 1.1, an excited pigment molecule can return to its stable state by transferring the energy to another pigment (e.g. LHC pigments), by transferring an electron to another molecule in primary charge separation, reversing its electron spin from singlet to triplet state or by releasing the excitation as heat. In addition, the excitation can be released as a photon i.e. by emitting fluorescence. At room temperature, fluorescence is mainly emitted from chlorophyll pigments associated with PSII, due to restrictions in forwarding their excitation energy to  $Q_A$  (Duysens and Sweers, 1963; Butler, 1972). Since the PQ pool is central in modulating the electron transfer rate, activating STN7 and receiving electrons from the cyclic pathway, chlorophyll fluorescence methods are extensively used to study the function of the ETC and the distribution of excitation energy. For the same reason, it was also the most important method used in this thesis.

To investigate the relative excitation between PSII and PSI, the chlorophyll fluorescence at 77 K (Paper I and IV) and 253 K (Paper IV) was monitored. Due to the rapid electron transfer from  $P700^+$  to the electron acceptors (Dau, 1994), only 10 % of total chlorophyll fluorescence derives from PSI-LHCI at 253 K (Govindjee, 1995), whereas freezing the thylakoids to 77 K halts any vibrational energy transfer between the pigments and thus multiplies the fluorescence emission from PSI-LHCI (Mukerji and Sauer, 1989). The samples in Paper I were prepared by diluting fractionated thylakoid membranes with the 25BTH20G buffer to a concentration of 2  $\mu\text{g}$  chlorophyll  $a+b$  / 100  $\mu\text{l}$ , and the samples in Paper IV by adding storage buffer to isolated thylakoids to a final concentration of 4  $\mu\text{g}$  chlorophyll  $a+b$  / 100  $\mu\text{l}$ . The samples were excited with 482.5 nm light and fluorescence emission was recorded using the Ocean Optics S2000 spectrophotometer. During the measurements, the samples were kept in a cold block (253 K,  $-20^\circ\text{C}$ ) or submerged into liquid nitrogen (77 K,  $-196^\circ\text{C}$ ).

In Papers II, III and IV, Dual pulse amplitude modulated (Dual-PAM) measuring system was used to acquire more detailed information on the functional photosystems. The system uses two separate light sources: actinic light (620 nm in this thesis), which drives photosynthesis, and a pulsing measuring beam, which induces PSII fluorescence at  $>700$  nm and PSI absorption change at 830 nm (Schreiber et al., 1986; Klughammer and Schreiber, 1994; Klughammer and Schreiber, 2008). By detecting only signal triggered by the measuring beam, actinic light intensities can be increased to a high level, and even pulses saturating the photosystems can be applied without discrepancies in the detection. At the beginning of a typical Dual-PAM experiment (Figure 4), minimal fluorescence ( $F_0$ ) is detected from plants acclimated to the dark. Next, a saturating flash is applied, resulting in maximal PSII fluorescence ( $F_M$ ). Maximal P700 signal ( $P_M$ ), on the other hand, is

## METHODOLOGY

obtained by applying a saturating flash after a period of far-red light that completely oxidizes PSI. More variables are collected after switching on actinic light:  $F'$  and  $P'$  refer to steady-state and  $F_M'$  and  $P_M'$  to maximal fluorescence and P700 signal under actinic light (Figure 4). With the variables –  $F_0$ ,  $F_M$ ,  $P_M$ ,  $F'$ ,  $P'$ ,  $F_M'$  and  $P_M'$  – several parameters can be calculated that describe the function of photosynthetic light reactions (Table 1).

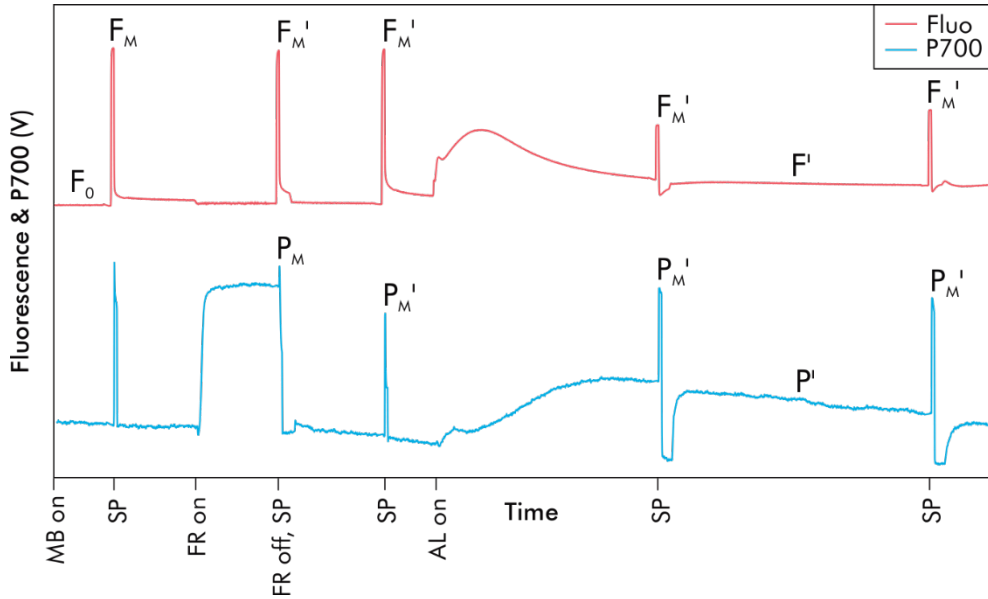


**Figure 4. Typical Dual-PAM measurement.** First, minimal fluorescence is detected under measuring beam (MB). High intensity saturating pulse (SP) is applied to yield maximal fluorescence ( $F_M$ ). Far-red light (FR) is turned on to determine maximal oxidation of P700 ( $P_M$ ) with another SP. Steady-state fluorescence and P700 under actinic light (AL) are designated as  $F'$  and  $P'$ , while the maximal values under AL as  $F_M'$  and  $P_M'$ . Figure is modified from Figure 1A in Paper II.

**Table 2. Dual-PAM parameters used in this thesis.**

Parameter	Definition
$F'/F_M$	$F'$ normalized to $F_M$ , relative reduction of $Q_A$ (Grieco et al., 2012)
$(F_M' - F')/F_M'$	Effective quantum yield of PSII (Genty et al., 1989)
$F_M'/F_M$	Photochemically active PSII (Paper II)
$1 - F_M'/F_M$	Non-photochemical quenching of fluorescence (Paper II)
$F_V/F_M$	$(F_M - F_0)/F_M$ , maximal quantum yield of PSII (Kitajima and Butler, 1975; Genty et al., 1989)
ETR(II)	Electron transfer through PSII, $[(F_M' - F')/F_M'] \times \text{PPFD} \times 0.84 \times 0.5$ (Miyake et al., 2005)
Y(NA)	$P_M - P_M'/P_M$ , acceptor side limitation of PSI (Klughammer and Schreiber, 1994; Klughammer and Schreiber, 2008)
Y(ND)	$P'/P_M$ , oxidation state or donor side limitation of PSI (Klughammer and Schreiber, 1994; Klughammer and Schreiber, 2008)
ETR(I)	Electron transfer through PSI, $[(P_M' - P')/P_M'] \times \text{PPFD} \times 0.84 \times 0.5$ (Miyake et al., 2005)

## 4 Results

### 4.1 Phosphorylation-dependent rearrangements in the PSII–LHCII–PSI–LHCI megacomplex

#### 4.1.2 L-LHCII connects the differently localized photosystems

To examine the functional interactions between the differently localized protein complexes, in Paper I, thylakoid fractions with different protein complexes composition were created by dissecting the thylakoids with (i) digitonin, (ii) DM or (iii) digitonin followed by DM. Notably, both the solubilized and insolubilized fractions were analysed in respect to their protein complex composition as well as their relative distribution of excitation energy between PSII and PSI (Figure 5). Protein complexes in the intact thylakoid (Intact) as well as in the insoluble fractions after treatment with digitonin (DIG P) or DM (DM P) failed to penetrate the stacking gel and were left in the well (Figure 5A). The solubilized fractions after digitonin (DIG S) and DM (DM S) treatment, on the other hand, showed the typical protein complex pattern described by Järvi et al., 2011. Digitonin detached the large PSII–LHCII–PSI–LHCI megacomplex, smaller PSII–LHCII supercomplexes, the so called ‘state transition complex’ PSI–LHCII, monomeric PSI, dimeric and monomeric PSII, ATP synthase, Cyt  $b_6f$  as well as free L-LHCII (DM S). DM, on the other hand, disintegrated four PSII–LHCII supercomplexes, monomeric PSI, dimeric and monomeric PSII, M- and L-LHCII as well as monomeric LHCII proteins (DM S).

DM is capable of dissecting almost the whole membrane into small complexes and was, for this reason, used to further open the digitonin fractions. Indeed, DM was able to detach the PSII–LHCII and M- and L-LHCII complexes from the grana core (DIG P + DM) and, intriguingly, to disassemble the large PSII–LHCII–PSI–LHCI megacomplex in the non-appressed membranes into PSII–LHCI, L-LHCII and photosystems (DIG S + DM) (Figure 5A). Importantly, the DM solubilization of both digitonin fractions was accompanied by fluorescence emission at 680 nm (Figure 5B) – wavelength attributed to L-LHCII (Figure 2E in Paper I). Together, the results from the BN-PAGE (Figure 5A) and fluorescence spectra (Figure 5B)

## RESULTS

suggest that the PSI–LHCI complexes form large megacomplexes with the grana-enriched PSII–LHCII and that this connection is mediated by L-LHCII.

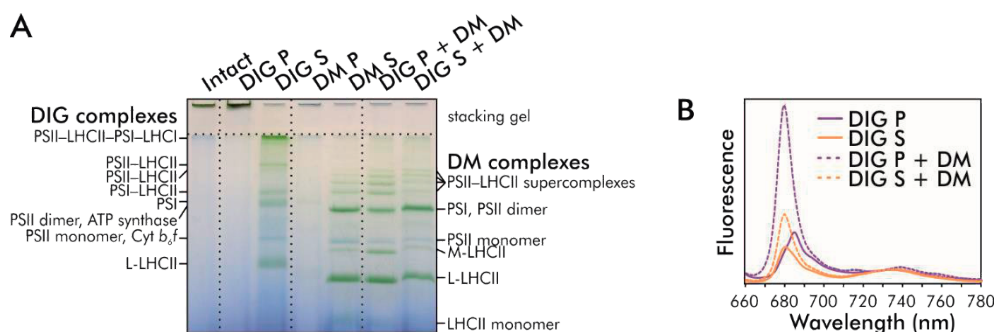


**Figure 5. Protein complex composition and relative excitation balance in thylakoid fractions obtained with digitonin.** Thylakoids were isolated from WT plants grown in moderate growth light ( $120 \mu\text{mol photons m}^{-2} \text{s}^{-1}$ ) and solubilized with either 1 % digitonin (DIG) or 1 % DM. The soluble supernatant (S) and the insoluble pellet (P) fractions were then separated with centrifugation at  $18,620 \times g$ , and the S and P from DIG solubilization were further treated with 1 % DM (DIG P + DM and DIG S + DM). **(A)** Serva Blue G buffer was added to a final volume of 10 % (v/v) and the samples ( $1 \mu\text{g}$  of chlorophyll *a+b*) were analyzed with IpBN-PAGE with an acrylamide gradient of 3–12.5 %. **(B)** Thylakoid fractions were diluted into  $2 \mu\text{g}$  chlorophyll /  $100 \mu\text{l}$ , and fluorescence at 77 K was detected. Data were normalized to 733 nm. Figure is modified from Figure 2 in Paper I.

### 4.1.2 Phosphorylation status of LHCB2 determines the association of PSI in the large megacomplex at grana margins

Since L-LHCII was demonstrated to energetically connect the protein complexes between the appressed and nonappressed membranes, the reversible phosphorylation of LHCB1 and LHCB2 likely plays a central role in regulating the interactions. To investigate the means of such regulation, growth light and high light acclimated and thus differently phosphorylated WT, *stn7*, *stn8*, *stn7stn8* and *tap38/pph1* thylakoids were solubilized with digitonin. Moreover, to follow the disintegration of the PSII–LHCII–PSI–LHCI megacomplex, the digitonin concentration was gradually increased and again, both the soluble and insoluble fractions were analysed from each digitonin concentration.

The detachment of the different protein complexes of WT is depicted in Figure 6. Under growth light conditions, the first protein complexes to detach from the thylakoid membrane were Cyt  $b_6/f$  and ATP synthase, which were completely solubilized with 0.5 % digitonin. Next, PSI and phosphorylated LHCB2 (P-LHCB2) were fully disintegrated with 1 % digitonin. PSII, on the other hand, was practically insoluble. After acclimation to high light ( $600 \mu\text{mol photons m}^{-2} \text{s}^{-1}$  for 2 h), the detachment pattern drastically changed: now the majority of Cyt  $b_6/f$  and ATP



## RESULTS

synthase were solubilized with as low as 0.25 % digitonin and most of the PSI and P-LHCB2 already with 0.5 % digitonin. Under high light, PSII still remained unreachable for digitonin. Intriguingly, the other LHCB proteins studied (LHCB1, P-LHCB1, LHCB2 and LHCB3) behaved like P-LHCB2 under growth light, while as a response to the high light treatment, they were confined into the grana core (Figure 5B in Paper I).

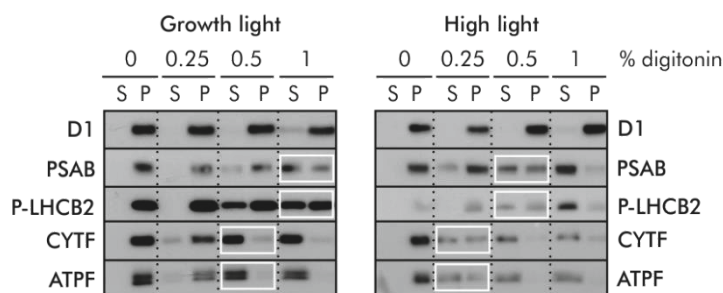


**Figure 6. Phosphorylation-dependent division of thylakoid protein complexes between appressed and non-appressed membranes under growth light and high light conditions.** Thylakoids were isolated from WT plants grown in moderate growth light ( $120 \mu\text{mol photons m}^{-2} \text{s}^{-1}$ ) as well as from plants treated with high light ( $600 \mu\text{mol photons m}^{-2} \text{s}^{-1}$  for 2 h), and the isolated thylakoids were submitted for solubilization with either 0.25, 0.5 or 1 % digitonin. The soluble supernatant (S) and the insoluble pellet (P) fractions were then separated with centrifugation at  $18,620 \times g$ , after which the proteins of the fractions were denatured and solubilized with sample buffer and separated with SDS-PAGE. Quantity of D1, P-LHCB2, PSAB, CYT F and ATP F, representing PSII, L-LHCII, PSI, Cyt b<sub>6</sub>f and ATP synthase were determined with specific antibodies. The white boxes indicate the digitonin concentration required to solubilize  $\geq 50$  % of the total amount of the protein.

The knock-out mutants *stn7*, *stn7stn8* and *tap38/pph1* explained the results gained from studying the WT. In the absence of STN7 and consequent LHCB phosphorylation (*stn7* and *stn7stn8*), the capability of digitonin to detach PSI, Cyt b<sub>6</sub>f and ATP synthase was facilitated under growth light intensity, whereas the opposite was true in the absence of TAP38/PPH1 (*tap38/pph1*) under high light (Figure 5A in Paper I). The chlorophyll *a/b* values correlated with the location of PSI: the chlorophyll *a/b* value significantly increased in the soluble fraction of *stn7* and *stn7stn8* under growth light and, conversely, in the insoluble fraction of *tap38/pph1* under high light conditions (Figure 3 in Paper I). When compared to PSI, Cyt b<sub>6</sub>f and ATP synthase, the LHCB2 protein remained relatively confined in the insoluble fraction in *stn7* and *stn7stn8* under growth light, whereas in *tap38/pph1* under high light it solubilized more readily (Figure 5B in Paper I). Under high light, the other LHCB isoforms – LHCB1, P-LHCB1, P-LHCB2 and LHCB3 – were packed in the insoluble fraction and were detachable only in *tap38/pph1* (Figure 5B in Paper I). As summarized in Figure 6, altogether the results from WT and the mutants demonstrate that the lateral heterogeneity between PSII and PSI along with

## RESULTS

Cyt  $b_6f$  and ATP synthase strengthens as a response to increasing light intensity in a process that is dependent on the reversible phosphorylation of LHCB2. Only PSII–LHCII complexes with phosphorylated LHCB2 seemed to interact with PSI and, intriguingly, this phosphorylation affected the rearrangements of the whole LET complex – including Cyt  $b_6f$  and ATP synthase.

### 4.2 Dependency of Dual-PAM parameters on light intensity and regulatory mechanisms

Photosynthetic light reactions are widely studied using Dual-PAM parameters, but detailed data on the dependency of the parameters on the molecular regulatory mechanisms of the ETC has been missing. Since the regulatory mechanisms function depending on the prevailing light conditions, the aim in Paper II was to determine which changes in fluorescence and P700 parameters are specific, on one hand, to the growth and actinic light intensity used in the measurements and, on the other hand, to the well-known ETC regulatory mutations used here to assist in the identification of the relationship between the molecular regulatory mechanisms and the biophysical parameters.

#### 4.2.1 Biophysically determined redox state of ETC is directly dependent on the growth light intensity

To investigate the effect of the growth and actinic light intensity on the Dual-PAM parameters, WT plants were grown under a low, moderate or high light intensity (50, 120 or 500 photons  $m^{-2} s^{-1}$ ) and were then subjected to Dual-PAM experiment with actinic light intensity growing in five steps (23, 54, 127, 532 and 1595 photons  $m^{-2} s^{-1}$ ). During the increase in actinic light intensity, the relative redox state of  $Q_A$ , estimated based on parameter  $F'/F_M$ , remained quite stable regardless of the preceding growth light intensity (Figure 3A in Paper II). In contrast, the photochemically active PSII ( $F_M'/F_M$ ) and the effective quantum yield of PSII ( $(F_M' - F^2)/F_M'$ ) (Genty et al., 1989) of the low-light-grown plants were saturated immediately after the actinic light intensity exceeded the light intensity the plants were grown under (Figure 3B and D in Paper II). Plants grown under moderate or high light reacted surprisingly similarly, by decreasing the fraction of photochemically active PSII and the effective quantum yield of PSII only under high light intensities. Similarly, the capacity to induce the thermal dissipation of excess excitation energy ( $1 - F_M'/F_M$ ) was dependent on the growth light intensity: the majority of fluorescence was non-photochemically quenched after the actinic light intensity exceeded that of growth light (Figure 3C in Paper II).

## RESULTS

Redox state of PSI was estimated with parameters Y(ND) and Y(NA), describing the donor and acceptor side limitation of PSI (Klughhammer and Schreiber, 1994; Klughhammer and Schreiber, 2008). The acceptor side limitation Y(NA) was kept relatively stable in all plants and conditions, while the donor side limitation Y(ND), describing the P700 oxidation state, increased immediately after the actinic light intensity exceeded that of growth light (Figure 6, left panel). Interestingly, the higher the growth light intensity was, the lower the capacity for the stromal electron acceptors to oxidize P700 under high actinic light remained. Together the behaviour of the fluorescence and P700 parameters demonstrate that growth light conditions have a considerable effect on the redox state of the ETC and, furthermore, on the redox state and capacity of the stromal acceptors. Consequently, the growth light conditions also have a profound impact on the Dual-PAM measurements. For this reason, when studying the molecular mechanisms using mutant lines, only plants grown under exactly the same conditions should be compared.

### 4.2.2 Reversible phosphorylation, thermal dissipation and PGR5-dependent control optimize the redox state of ETC

To elucidate how the regulatory mechanisms affect the Dual-PAM parameters, the behaviour of WT plants grown under low, moderate or high light intensity (50, 120 or 500 photons  $\text{m}^{-2} \text{s}^{-1}$ ) was compared with moderate-light-grown regulatory mutants lacking STN7 (*stn7*), TAP38/PPH1 (*tap38/pph1*), PGR5 (*pgr5*), PSBS (*npq4*) as well as both PSBS and STN7 (*npq4stn7*). As above, the parameters were detected under stepwise-increasing actinic light intensity (23, 54, 127, 532 and 1595 photons  $\text{m}^{-2} \text{s}^{-1}$ ). As to PSI, the absence of reversible LHCII phosphorylation caused notable changes in parameters Y(NA) and Y(ND) under low actinic light (Figure 6, right panel). Under low light, PSI was limited by the acceptor side in *stn7* and by the donor side in *tap38/pph1*, highlighting the role of steady-state phosphorylation in balancing the excitation energy between PSII and PSI. Unexpectedly, when the actinic light intensity exceeded that of growth light, the differences between *stn7* and *tap38/pph1* disappeared, suggesting the presence of another mechanism that protects PSI from photodamage under high light. Indeed, the additional lack of PSBS in the *stn7* mutant (*npq4stn7*) led to a more reduced P700 and allowed the acceptor side of PSI to limit also under high light. More severely, however, the Y(ND) and Y(NA) parameters were affected in *pgr5*, which showed substantial acceptor side limitation and was completely unable to oxidize P700 under actinic light intensities higher than the growth light.

With respect to fluorescence parameters  $F'/F_M$  and  $1-F_M'/F_M$ , the mutants *pgr5*, *npq4* and *npq4stn7* behaved very similarly (Figure 4 in Paper II). In the mutants, the PQ pool was seen to be relatively reduced, and the induction of thermal dissipation

## RESULTS

was weak under actinic light intensities exceeding the growth light intensity. This result indicates that both PGR5 and PSBS-dependent mechanisms are needed for the optimal oxidation of the PQ pool under high light. However, the absence of PSBS mostly only affected the fluorescence parameters, whereas the lack of PGR5 also disturbed the P700 parameters (Figure 7, right panel). Indeed, as reported in Papers II and III, the P700 of *pgr5* remains completely reduced under high light, whereas, interestingly, it is even more oxidized in *npq4* than in the WT (Figure 7A, right panel). This result demonstrates that under high light, the PSBS-dependent thermal dissipation of excess excitation energy from LHCII is insufficient to keep PSI oxidized, but instead, the PGR5-dependent mechanism is essential to protect the entire ETC from over-reduction.

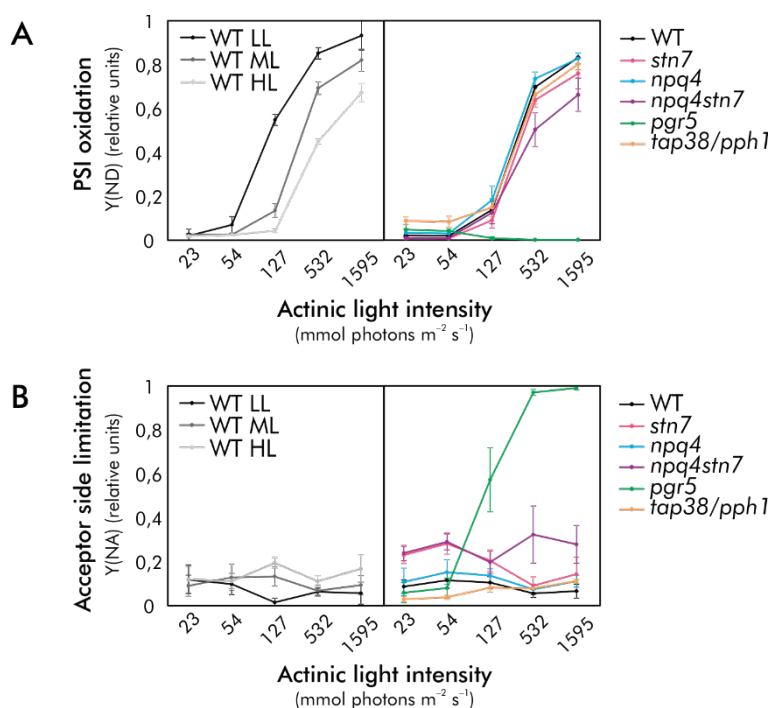


**Figure 7. Regulatory proteins STN7, TAP38, PSBS and PGR5 maintain optimal oxidation of PSI.** (A) Oxidation status and (B) acceptor side limitation of PSI, measured as Y(ND) and Y(NA), respectively, were recorded, while increasing actinic light intensity stepwise (23, 54, 127, 532, 1595 mmol photons m<sup>-2</sup> s<sup>-1</sup>), from *Arabidopsis thaliana* WT grown under low light (LL, 50 photons m<sup>-2</sup> s<sup>-1</sup>), moderate light (ML, 120 mmol photons m<sup>-2</sup> s<sup>-1</sup>) and high light (HL, 500 mmol photons m<sup>-2</sup> s<sup>-1</sup>) as well as from mutants *stn7*, *npq4*, *npq4stn7*, *pgr5* and *tap38/pph1* grown under moderate light. The leaves were illuminated with each actinic light intensity for 5 min before applying the saturating pulse. Averages and standard deviations from 3–4 replicates are shown.

## RESULTS

### 4.2.3 PSI photoinhibition may affect the interpretation of fluorescence parameters

As explained above, *pgr5* is able to keep the ETC optimally oxidized under actinic light intensities that are lower or similar to that of the growth light, whereas any increase in the actinic light intensity severely disturbs the balance and is reflected in both fluorescence and P700 parameters (Figure 4 in Paper II). If the actinic light intensity fluctuates between low and high, the mutant is unable to control the electron flow from PSII to PSI, which leads to the inhibition of PSI (Suorsa et al., 2012). Interestingly, the maximal quantum yield of PSII, measured as  $F_v/F_M$  (Kitajima and Butler, 1975; Genty et al., 1989), was decreased in *pgr5* grown three days under fluctuating light, suggesting photoinhibition also at PSII. However, parameter  $F_v/F_M$  is derived from  $(F_M - F_0)/F_M$ , and when the variables  $F_M$  and  $F_0$  were individually analyzed, PSII ( $F_M$ ) was confirmed to be unaffected. Instead,  $P_M$  was seen to be drastically decreased and, conversely,  $F_0$  substantially increased, indicating that the limited amount of functional PSI centres accumulates electrons in the PQ pool and consequently raises the baseline fluorescence  $F_0$ . This result implies that, in some cases, the treatment of the raw signals such as  $F_0$  and  $F_M$  can mask valuable information and, for this reason, special caution should be exercised when calculating parameters for regulatory mutants with an unknown molecular phenotype.

### 4.3 Role of PGR5 and NDH-1 in protecting PSI from photoinhibition

Papers II and III demonstrated that under any increase in light intensity, the PGR5-dependent regulatory mechanism keeps P700 oxidized by preventing excess electrons from over-reducing the electron acceptors of PSI. In Paper IV, the capacity of PGR5 to protect PSI from damage upon a sudden increase in light intensity was compared to that of NDH-1 mediating CET and chlororespiration. To this end, PSI of the WT, *pgr5* and *ndho* was specifically run down with a series of light treatments, which involved first reducing the ETC with red light and then saturating the PSI electron acceptors with a high-intensity pulse of white light (Tikkanen and Grebe, 2018). Furthermore, the possible role of PGR5 and NDH-1 in mitigating the consequences of PSI inhibition was investigated. For this reason, before any experiments, the plants were allowed to re-balance their photosynthetic machinery to the new PSI-limiting state for 24 h, during which the inhibited PSI is unable to recover (Lima-Melo et al., 2018; Tikkanen and Grebe, 2018).

## RESULTS

### 4.3.1 PGR5 and NDH-1 are unable to protect PSI by accepting electrons upon a sudden increase in light intensity

First, to compare the capacity of PGR5 and NDH-1 to protect PSI against the photoinhibition treatment, the functional and actual amount of PSII and PSI were determined using Dual-PAM and EPR (Figure 2A and B in Paper IV). Unexpectedly, the decreasing maximal fraction of photo-oxidable PSI,  $P_M$ , demonstrated that the inhibition treatment affected WT, *pgr5* and *ndho* very similarly (Figure 8, left panel). Notably, only the function of PSI was run down, while the functional PSII as well as the total amount of both photosystems remained unaffected (Figure 2C in Paper IV). The result indicates that neither PGR5 nor NDH-1 are capable of protecting PSI by accepting electrons upon a sudden increase in light intensity if the electrons have already accumulated in the ETC, as is the case after the deliberate PSI photoinhibition treatment. To confirm that the intriguing result actually derives from the inability of PGR5 and NDH-1 to quickly accept electrons from PSI, *Physcomitrella patens* WT and *flvb* mutant were added to the analysis. The *flvb* mutant lacks both the FLV proteins known to protect PSI of *Physcomitrella patens* by safely scavenging electrons upon an increase in light intensity (Gerotto et al., 2016). Indeed, only *Physcomitrella patens* WT with functional FLV proteins was tolerant to the inhibitory treatment, while the *flvb* mutant behaved like the *Arabidopsis thaliana* WT and mutants by showing a significant decrease in the  $P_M$  value (Figure 8, right panel), while  $F_M$  remained unaffected (Figure 2D in Paper IV).

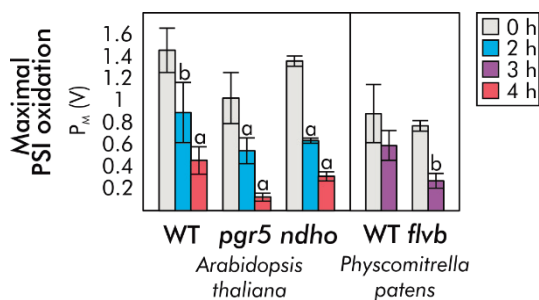


**Figure 8. Fraction of functional PSI after deliberate photoinhibition treatment.** The maximal oxidation level of PSI,  $P_M$ , was determined from *Arabidopsis thaliana* WT, *pgr5* and *ndho* leaves and from *Physcomitrella patens* WT and *flvb* mutant protonemal tissue after 0, 2, 3 and 4 h of PSI photoinhibition treatment. Before the experiments, the treated samples were allowed to rebalance their photosynthetic machinery for 24 h under growth light conditions before any experiments. Averages of 3–5 measurements are shown with their standard deviations. Statistical significance between the samples was determined with one-way ANOVA and Tukey's test. Significant differences between the control (0 h) and photoinhibited (2 h and 4 h) samples are shown with letters a and b, referring to  $p < 0.01$  and  $p < 0.05$ , respectively.

## RESULTS

### 4.3.2 Mobile electron carriers and PGR5-dependent photosynthetic control maintain ETC after PSI photoinhibition

Since PGR5 and NDH-1 were concluded to be unable to protect PSI by accepting electrons, their possible roles in rebalancing the ETC after the PSI photoinhibition was investigated next. To this end, the electron transfer rate through the photosystems of WT, *pgr5* and *ndho* was estimated with Dual-PAM parameters ETR(II) and ETR(I), introduced by Miyake et al. 2005, after 1 min of low ( $50 \mu\text{mol photons m}^{-2} \text{s}^{-1}$ ) and high ( $600 \mu\text{mol photons m}^{-2} \text{s}^{-1}$ ) red actinic light illumination differently oxidizing the ETC (For light treatment details, see Table 2 in Paper IV). Remarkably, under low actinic light, the decreased amount of functional PSI drastically decelerated the electron transfer through PSII and accelerated that through PSI in all genotypes (Figure 9, left panel). Under high actinic light, on the other hand, clear genotype-specific differences emerged: as the PSI photoinhibition proceeded, the ETR(II) slightly decreased in *pgr5* but remained relatively high in WT and *ndho*, while, intriguingly, the ETR(I) increased as high as threefold in WT and fourfold in *ndho*, but remained unaffected in *pgr5* (Figure 9, right panel). The behaviour of the ETR(II) parameter demonstrates that PGR5 is necessary to the modulating of electron transfer through PSII under high light and that its function is completely independent of the amount of functional PSI. Moreover, the ETR(I) results suggest that the PGR5-dependent control of electron flow from PSII to PSI enables the functional PSI centres to accelerate their electron transfer in order to compensate for the lost photosystems.

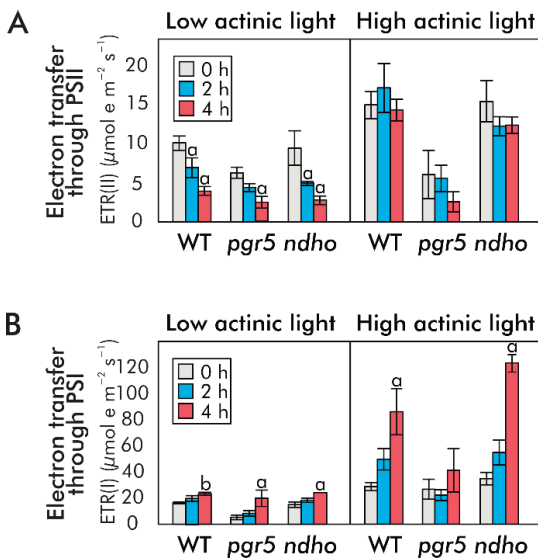


**Figure 9. Electron transfer through photosystems after PSI photoinhibition.** Electron transfer rate (ETR) through PSII and PSI in *Arabidopsis thaliana* WT, *pgr5* and *ndho* leaves after 0, 2 and 4 h PSI photoinhibition treatment was determined with Dual-PAM parameters (A) ETR(II) and (B) ETR(I), respectively, and after 1 min of low ( $50 \mu\text{mol photons m}^{-2} \text{s}^{-1}$ ) and high ( $600 \mu\text{mol photons m}^{-2} \text{s}^{-1}$ ) actinic light (AL). Before the experiments, the treated leaves were allowed to rebalance their photosynthetic machinery for 24 h under growth light conditions before any experiments. Averages of 3–5 measurements are shown with their standard deviations. Statistical significance between the samples was determined with one-way ANOVA and Tukey's test. Significant differences between the control (0 h) and photoinhibited (2 h and 4 h) samples are shown with letters a and b, referring to  $p < 0.01$  and  $p < 0.05$ , respectively.

## RESULTS

To elucidate this genotype-specific rate of electron transfer through the photosystems, more Dual-PAM parameters were calculated after 1 min of low and high actinic light differently oxidizing the ETC (For light treatment details, see Table 2 in Paper IV). The decreasing amount of functional PSI centres was visibly reflected in the redox state of the PQ pool, measured as  $F'/F_M$  (Figure 5C in Paper IV). Under low actinic light, the PQ pool of all genotypes became reduced as the amount of functional PSI centres significantly declined and, in line with the ETR(II), this phenomenon was the most prominent in *pgr5*. Under high actinic light, the activated photosynthetic control and thermal dissipation in WT and *ndho* were able to prevent the further reduction of the PQ pool despite the PSI photoinhibition, whereas the PQ pool of *pgr5* gradually became reduced under these conditions, eventually saturating both the donor and acceptor sides of PSI (Figures 5A–B in Paper IV) and slowing down the electron transfer through PSII (Figure 9A, right panel).

The donor and acceptor side limitation of PSI, measured as parameters Y(ND) (Figure 10A) and Y(NA) (Figure 5B in Paper IV), might explain the genotype-specific differences in electron transfer through PSI. Under low light, the PSI inhibition drastically decreased both the donor and acceptor side limitation of PSI in WT, *pgr5* and *ndho*, suggesting that the still functional PSI centres receive relatively more electrons at the donor side and relatively more free electron acceptors at the acceptor side of PSI. Under high light, on the other hand, the decrease in the amount of functional PSI centres enabled the PGR5-dependent mechanism and the thermal dissipation to enhance the oxidation of P700 in WT and especially in *ndho*, resulting in increased donor side limitation and decreased acceptor side limitation i.e. in more prominent photosynthetic control. Interestingly, the improved oxidation was accompanied by an increased amount of PGR5 as a response to PSI photoinhibition (Figure 10B). Evidently, the enhanced capacity for photosynthetic control had no effect on PSI oxidation under far-red actinic light, but it could explain why WT and especially *ndho* were able to oxidize their PSI under high light – even more effectively after PSI photoinhibition (Figure 10A). In addition, some NDH-1-dependent oxidation was seen under high light before the photoinhibitory treatments, after which the PGR5-dependent mechanism took over. The results suggest that, under light-limiting conditions, electron transfer from PSII to PSI is dependent on the availability of mobile electron carriers that reduce and oxidize PSI, whereas under excess light, the rate is modulated by PGR5.

### 4.3.3 NDH-1 and PTOX protect PSI from over-reduction by enhancing the proton gradient with chlororespiration

A possible role for NDH-1 in the mitigation of the consequences of PSI photoinhibition was found when the Y(ND) parameter, describing the redox state of



## RESULTS

PSI, was calculated after 1 min of far-red light (Figure 10A). The strong genotype-dependent behaviour of Y(ND) under far-red light demonstrated that, although far-red light specifically excites and thus oxidizes PSI, the decreasing amount of functional PSI leads to accumulation of the electrons from PSII in the ETC, seen as a reduced P700 i.e. low Y(ND). The capacity of far-red light to oxidize PSI was weakened in the absence of NDH-1 and conversely increase in the absence of PGR5. This surprising result suggests that NDH-1 might have a CET-independent role in oxidizing the ETC and that this mechanism could be enhanced in the absence of PGR5. Subsequent western blotting (Figure 10B) provided further evidence for the hypothesis by revealing that, indeed, NDH-1 and PTOX are upregulated in *pgr5*, which means that it is conceivable for the proton-gradient-generating chlororespiration to maintain P700 predominantly oxidized even in *pgr5* under far-red illumination.

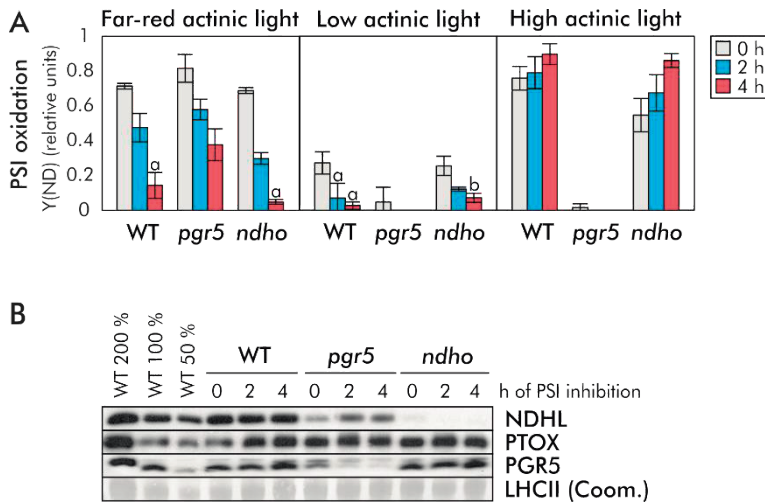


**Figure 10. PSI oxidation depends on chlororespiration under far-red light and on PGR5 under high light.** **A.** Oxidation of PSI measured as Dual-PAM parameter Y(ND)=P/P<sub>M</sub> was determined from WT, *pgr5* and *ndho* leaves after 0, 2 and 4 h of PSI inhibition treatment and after far-red, low intensity (50  $\mu\text{mol photons m}^{-2} \text{s}^{-1}$ ) and high intensity (600  $\mu\text{mol photons m}^{-2} \text{s}^{-1}$ ) actinic light. Averages of 3–5 measurements are shown with their standard deviations. **B.** Proteins from the isolated thylakoid membranes of WT, *pgr5* and *ndho* after 0, 2 and 4 h of PSI inhibition were separated with SDS-PAGE, transferred to a PVDF membrane and immunodetected with antibodies against NDHL, PGR5 and PTOX. Equal sample loading was confirmed with Coomassie (Coom.) staining. After photoinhibitory treatments, the plant leaves were allowed to rebalance their photosynthetic machinery for 24 h under growth light conditions before any experiments. Statistical significance between the samples was determined with one-way ANOVA and Tukey's test. Significant differences between the control (0 h) and photoinhibited (2 h and 4 h) samples are shown with letters a and b, referring to  $p < 0.01$  and  $p < 0.05$ , respectively.

## RESULTS

### 4.3.4 Light-activated PGR5 efficiently protects PSI from further damage under high light

To take a closer look at the PGR5 mechanism, the kinetics of P700 oxidation during a high-intensity pulse of white light were dissected (Figure 11). The rapid oxidation of WT P700 upon the saturating pulse indicated that the PGR5-dependent mechanism can respond to an increase in light intensity as quickly as in milliseconds (Figure 11, lower panel). However, the similar oxidation capacity of WT and *pgr5* after dark acclimation revealed that, in order to protect PSI against the sudden increase in light intensity, PGR5 first requires activation by light (Figure 11, upper panel). Nevertheless, as the PSI photoinhibition proceeded, the electrons accumulating in the ETC during the low red actinic light drastically decreased the capacity of PGR5 to oxidize P700 upon the saturating pulse (Figure 11, lower panel). Since the photosynthetic control remained inactive under low actinic light ( $F'/F_M$ , Figure 5C in Paper IV), this demonstrates that PGR5 is incapable of protecting PSI upon increasing light intensity if electrons have already accumulated in the ETC.

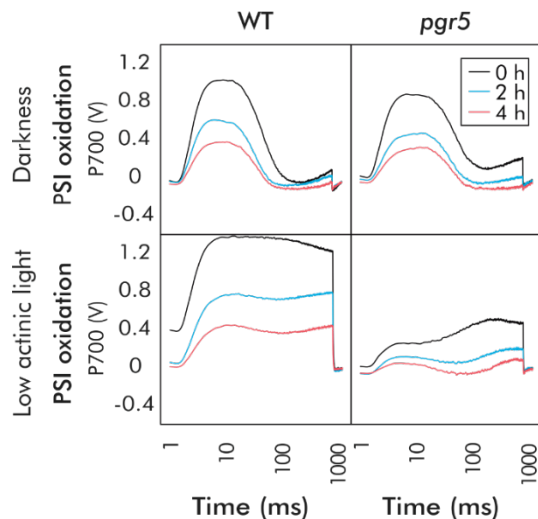


**Figure 11. PGR5-dependent oxidation of PSI upon abrupt increase in light intensity.** P700 kinetics during saturating pulse were detected from the WT and *pgr5* after 0, 2 and 4 h of PSI inhibition and after (A) 10 min dark acclimation and (B) 1 min of low ( $50 \mu\text{mol photons m}^{-2} \text{s}^{-1}$ ) red actinic light. Before the experiments, the treated samples were allowed to rebalance their photosynthetic machinery for 24 h under growth light conditions. Data shown are averages of 3–5 independent measurements that were normalized to the final value at 1600 ms. Curves are presented on a  $\log_{10}$  scale.

## 5 Discussion

Natural fluctuations in light intensity challenge the photosynthetic light reactions, so to ensure efficient growth and development without wasting resources, plants are constantly balancing between maximal photosynthetic performance and minimal oxidative damage. While the progenitors of chloroplasts, the cyanobacteria, rely on electron scavengers and alternative electron transfer routes to protect their photosynthetic machinery from light-induced damage, during the evolution land plants have gradually changed their strategy from safety valves to preventing the over-reduction of PSI (Järvi et al., 2017). In order to protect PSI, flowering plants like *Arabidopsis thaliana*, have developed a variety of molecular regulatory mechanisms that optimize the distribution of excitation energy through reversible phosphorylation and thermal dissipation as well as modulate the intersystem electron transfer chain through photosynthetic control and chlororespiration. During the development of these mechanisms, the soluble phycobilisome antenna was also replaced with the membrane-bound LHCII antenna that enabled the thylakoid membrane to stack and to partially separate PSII from PSI (Anderson, 1982). The consequent two distinct thylakoid domains, the appressed and non-appressed membranes, are thought to ensure efficient energy harvesting and protection of both photosystems. In this thesis, *Arabidopsis thaliana* was used as a model organism to investigate the strategy used by the flowering plants to protect PSI from light-induced damage. The regulatory mechanisms were studied using a number of different biochemical and biophysical approaches that were applied to several lines of knock-out mutants lacking one or two of the regulatory proteins of photosynthetic electron transfer.

### 5.1 Phosphorylation-dependent protein complex rearrangements in the PSII-LHCII-PSI-LHCI megacomplex at the grana margins

The reversible phosphorylation of LHCII is known to optimize the distribution of excitation energy between PSII and PSI (Bellafiore et al., 2005; Pribil et al., 2010; Shapiguzov et al., 2010). Phosphorylated LHCB1 and LHCB2 subunits of LHCII increase the physical affinity between LHCII and PSI (Lunde et al., 2000; Bellafiore

## DISCUSSION

et al., 2005) and the resulting PSII–LHCII–PSI–LHCII megacomplexes have been found on the non-appressed regions (Suorsa et al., 2015). To investigate the energetic connectivity and phosphorylation-dependent rearrangements of the PSII–LHCII–PSI–LHCI megacomplex upon light acclimation, protein complexes on the non-appressed thylakoids were detached from the thylakoid membranes with an increasing digitonin concentration (Paper I). Since, traditionally, only the digitonin-solubilized fraction of the thylakoids has been analysed, valuable information on the physical interactions between protein complexes may have been ignored and, for this reason, the approach in Paper I was to biochemically and biophysically analyse both the soluble and the insoluble fractions after digitonin solubilization. It is important to note that the gradual access of digitonin into the thylakoid protein complexes is likely based on stepwise breakage of interactions between the subcomplexes, rather than actually steadily approaching the grana core as schematically depicted in Figure 3.

### 5.1.1 Phosphorylation status of LHCB2 determines the association of PSI in the megacomplex

Under growth light conditions, WT plants show a moderate phosphorylation level of the PSII core proteins D1, D2 and CP43 as well as the LHCII proteins LHCB1 and LHCB2, while an increase in light intensity enhances the phosphorylation of the PSII core and minimizes that of the LHCII proteins (Figure 1A in Paper I). Intriguingly, the light-intensity-dependent phosphorylation status was accompanied by a specific digitonin-dependent detachment pattern (Figure 6) of the protein complexes based on their distribution in the thylakoid membrane (Figure 2). Indeed, as a response to the increased light intensity, also the protein complexes underwent very distinct rearrangements: under high light, both PSII and dephosphorylated LHCB2 were found enriched in the digitonin-insoluble fraction, while the solubilization of PSI along with a residual amount of P-LHCB2 was, interestingly, enhanced. Importantly, the high-light-induced rearrangements were completely dependent on the dephosphorylation of LHCII by TAP38/PPH1 (Figure 6). This result clearly demonstrates that the phosphorylation state of LHCB2 plays a major role in determining the availability of digitonin to detach PSI, which is well in line with the recent report demonstrating that it is L-LHCII that connects the PSII–LHCII complex to PSI at the grana margins (Rantala et al., 2017).

PSI bound to PSII via phosphorylated L-LHCII is difficult for digitonin to detach from the thylakoid membrane, as demonstrated by the ever-present residual PSI proteins (Figure 6) and PSI fluorescence in the digitonin-insoluble fraction (Figure 2B in Publication I) and in the grana fractions obtained with either digitonin or mechanical fractionation (Andreasson et al., 1988; Danielsson et al., 2004;

## DISCUSSION

Danielsson et al., 2006). As illustrated in Figure 12, this most likely results from the strong interaction between PSI and L-LHCII that confines PSI to the large PSII–LHCII–PSI–LHCI megacomplex and from the possible location of the megacomplex in the partly folded grana margins (Figure 2). Indeed, as a response to high light intensity, the dephosphorylation of L-LHCII releases PSI from the megacomplex and makes it more susceptible for digitonin (Suorsa et al., 2015), and, simultaneously, the high-level phosphorylation of PSII increases the stromal gap between the grana stacks (Fristedt et al., 2009) and exposes the grana-enriched complexes to digitonin (Figure 6).

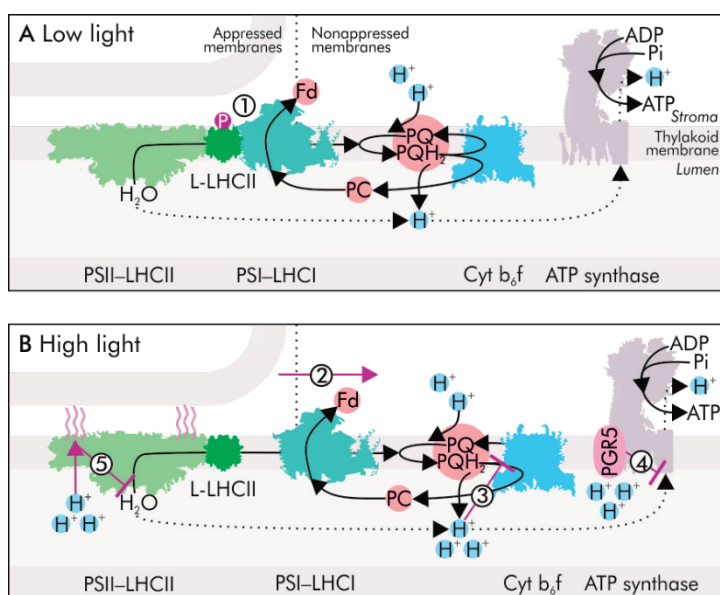


**Figure 12. LHCII phosphorylation, photosynthetic control and thermal dissipation of excess excitation energy in protecting PSI from excess electrons. A.** (1) Under low light, phosphorylation of L-LHCII binds PSII–LHCII and PSI–LHCI into one megacomplex, increasing the light harvesting antenna for PSI, which is the complex limiting the electron transfer rate. **B.** Increasing light intensity, however, induces several changes that protect PSI from excess electrons: (2) The STN7 kinase is inactivated and the TAP38/PPH1 phosphatase is able to dephosphorylate the L-LHCII. (3) The dephosphorylation of L-LHCII releases PSI–LHCI from the megacomplex and, simultaneously, the location of Cyt b<sub>6</sub>f and ATP synthase is also regulated. Increased light energy accelerates the electron transfer and consequently acidifies the thylakoid lumen. (4) The PGR5 protein maintains the generated proton gradient through a currently uncharacterized mechanism, thereby allowing the induction (5) of the photosynthetic control at Cyt b<sub>6</sub>f, limiting the electron transfer from PSII to PSI, (6) as well as of the thermal dissipation (wavy lines) of excess excitation energy at the LHCII antenna, which decelerates the electron transfer at PSII and thus alleviates the electron pressure at the PQ pool.

## DISCUSSION

### 5.1.2 STN7-dependent rearrangements over-ride any STN8-dependent changes in grana stacking

As a response to high light, grana stacks are loosened and the diameter of the stack decreases in a process that is dependent on STN8 kinase and the increased phosphorylation of PSII core proteins (Fristedt et al., 2009; Herbstová et al., 2012). The architectural alterations have been reported to facilitate the movement of photoinhibited PSII from the grana core to the non-appressed membranes for the replacement of the damaged D1 protein (Tikkanen et al., 2008; Fristedt et al., 2009). For this reason, digitonin in Paper I was expected to detach a larger fraction of the D1 protein after high light treatment and consequent PSII photoinhibition. Surprisingly, the opposite was observed, and the distribution of D1 protein remained unaltered after the high light treatment (Figure 6). However, unlike in the study completed by Fristedt et al., no inhibitors of D1 synthesis were used in Paper I, likely explaining the absence of D1 in the soluble fraction.

Another unexpected result was that the detachment pattern of the protein complexes from the thylakoid membrane in *stn8* resembled that in WT even after the high light treatment, where the WT and *stn8* show completely different membrane structure: narrow and loose grana stacks in WT and wide grana stacks with fewer layers in *stn8* (Fristedt et al., 2009). It is possible that, despite the drastically distinct membrane architecture, the two genotypes eventually contain a similar amount of digitonin-accessible membrane. Moreover, the protein complexes of the *stn7stn8* double mutant detached from the thylakoid membrane in the same way as in *stn7*, even though the grana stacks of *stn7stn8* show similar architecture as those in *stn8* (Fristedt et al., 2009), suggesting that the function of STN7 and TAP38/PPH1 likely over-rides the lack of STN8. This would also explain the similar distribution of excitation energy in WT, *stn8* and the mutant lacking PSII core phosphatase PBCP in both light conditions (Paper I; Mekala et al. 2015).

### 5.1.3 Similar light-intensity-dependent dynamics of PSI and Cyt b<sub>6</sub>f might protect PSI from photoinhibition

Despite extensive research, no consensus has been reached about the location of Cyt b<sub>6</sub>f in the thylakoid membrane. Spectrophotometric and immunological analyses of mechanically fractionated thylakoid membranes concluded Cyt b<sub>6</sub>f to reside slightly enriched in the grana vesicles containing both the grana core and margins (Andreasson et al., 1988). Nevertheless, later BN-PAGE analysis of similar fractions visualized the complex all over the thylakoid membrane, except for the Y-100 fraction, but mostly enriched in the stroma thylakoids and grana margins (Danielsson et al., 2006). Immunoblots of the soluble and insoluble digitonin fractions in Paper I, on the other hand, localize the complex explicitly on the non-appressed membranes

## DISCUSSION

under both growth light and high light, while only a residual amount of Cyt  $b_6f$  was left insoluble after as low as 0.5 % digitonin (Figure 6). In line with this result, it has been previously demonstrated that Cyt  $b_6f$  is enriched in the stroma thylakoids ( $150,000 \times g$  digitonin fraction) together with the STN7 kinase that relies on the complex for activation under low light (Wunder et al., 2013). On the other hand, the complex is an essential part of the photosynthetic light reactions and should, for this reason, be located close to the photosystems. The clear localization of Cyt  $b_6f$  in the stroma thylakoids (Wunder et al., 2013) may actually derive from the fact that the complex is not a physiological part of the PSII-LHCII-PSI-LHCII megacomplex (Rantala et al., 2017) and is therefore extremely susceptible to digitonin solubilization even at the grana margins (Figure 12).

Intriguingly, the gradual detachment of protein complexes from the thylakoid system revealed that the behaviour of Cyt  $b_6f$  followed that of PSI both under growth light and after high light treatment (Figure 6). Indeed, the fact that Cyt  $b_6f$  was found in the non-appressed membranes even under high light, when the increasing stromal gap would allow the flat complex to diffuse into the grana core, suggests that the complex might be under similar light-intensity-dependent regulation as the one that separates PSI from the megacomplex. In fact, the PETO subunit of Cyt  $b_6f$  has been shown to undergo reversible phosphorylation by the STN7 kinase homolog Stt7 as a part of the activation of the kinase in green algae *Chlamydomonas reinhardtii* (Hamel et al., 2000). Since the subunit is only loosely bound and not necessary for the enzymatic activity of the complex, it might serve a regulatory role in state transitions (Hamel et al., 2000). Moreover, similar function has been proposed for a loosely bound subunit Ssr2298 in cyanobacterium *Synechocystis* sp. PCC6803 (Volkmer et al., 2007). However, whether such subunits exist and regulate the distribution of excitation energy in plants remains to be solved.

The reason for the pronounced dynamics of the lateral heterogeneity of the thylakoid protein complexes as a response to increasing light intensity is still unclear, but, based on Papers I and IV, they might serve as a protective mechanism for PSI (Figure 12B). The dephosphorylation of LHCII upon an increase in light intensity undoubtedly decreases the fraction of LHCII collecting excitation energy for PSI, yet in the case of a sudden burst of electrons from PSII, a small antenna incapable of powering the electrons forward would be detrimental. Instead, according to the Papers II–IV, the protection of PSI in flowering plants is dependent on the ability to modulate electron transfer from PSII to PSI by PGR5. Thus, the protective effect provided by the dynamics of the lateral heterogeneity likely derives from the physical control of the distance between PSII, PSI and Cyt  $b_6f$  (Figure 12B). Similar regulation of PSI and Cyt  $b_6f$  could also allow a fast activation of the STN7 kinase on the onset of illumination, ensuring sufficient energy for the NDH-1-dependent

CET that, during the activation of carbon assimilation reactions, could prevent over-reduction of the stromal acceptors.

## 5.2 PGR5, NDH-1 and PTOX protect PSI from photoinhibition by modulating the proton gradient

It has been clearly demonstrated that PSI is extremely susceptible to excess electrons over-reducing and damaging its FeS centres (Sonoike, 1996; Sonoike, 2011; Suorsa et al., 2012). Excess electrons can accumulate when the light intensity suddenly increases and PSII feeds electrons to the ETC regardless of the redox state of PSI's stromal acceptors. Since light conditions in nature rarely remain constant, plants need to respond to fluctuations in light intensity very quickly in order to protect PSI from over-reduction and, since the light conditions in nature always coexist with various other abiotic and biotic factors, it is plausible that occasionally the regulatory mechanisms fail to keep the ETC optimally oxidized and PSI gets damaged. Due to the lack of an efficient repair cycle for the damaged PSI, plants have created an efficient regulatory network controlling the electron flow from PSII to PSI both in order to prevent and mitigate the photoinhibition of PSI.

In light of current knowledge, PGR5 and NDH-1 protect PSI from over-reduction by cycling electrons from ferredoxin to the PQ pool (Yamori and Shikanai, 2016). However, a comparison of the flowering plant *Arabidopsis thaliana* and the moss *Physcomitrella patens* with respect to their tolerance against PSI photoinhibition revealed that neither PGR5 nor NDH-1 can protect PSI upon a sudden over-reduction of its acceptor side, unlike the FLV proteins of *Physcomitrella patens* (Figure 8). The inability of NDH-1 to unload the electron pressure at PSI might simply result from too slow oxidation capacity or, alternatively, the FLV proteins might be able to accept their electrons directly from the FeS centres of PSI. For some reason, however, flowering plants lost the FLV proteins during their evolution and, as demonstrated in Papers II, III and IV, protect their PSI by optimizing the redox state of the ETC.

### 5.2.1 PGR5 only modulates the rate of CET indirectly

The *pgr5* mutant lacking the functional PGR5 protein was first identified for its reduced capacity to induce the thermal dissipation of excess excitation energy, and this defect was found to be connected to its extremely reduced ETC under high light (Munekage et al., 2002). The reduced ETC, on the other hand, was proposed to be result of an uncontrolled flow of electrons from PSII to PSI due to the lack of CET (Munekage et al., 2002). According to this view PGR5 would cycle electrons from PSI to the PQ pool, thus strengthening the proton gradient, and, consequently, induce



## DISCUSSION

thermal dissipation from the PSII antenna, finally preventing more electrons from entering the ETC (Munekage et al., 2002). In light of recent research, however, this model appears inconsistent. First, if CET were induced under excess light, it would work against photosynthetic control by activating the Q cycle; it therefore seems illogical for the oxidation of PSI to require further reduction of the ETC. Second, as also demonstrated in Paper I, it is now clear that LHCII can act as a shared antenna for both PSII and PSI (Wientjes et al., 2013a; Grieco et al., 2015; Akhtar et al., 2016; Bos et al., 2017; Rantala et al., 2017), making it impossible to specifically down-regulate PSII. In fact, in the absence of either the xanthophyll cycle (Grieco et al., 2012) or the PSBS protein (Papers II and III), PSI has been shown to receive extra energy and to be able to avoid over-reduction even under very high light.

A major leap towards disclosing the physiological role of PGR5 was taken when *pgr5* was found to be unable to survive sudden increases in light intensity due to its over-reduced ETC and consequently damaged PSI (Suorsa et al., 2012). Although the over-reduced PSI of *pgr5* can be restored with an alternative electron acceptor (Munekage et al., 2002), it is also possible to achieve the same result with DCMU treatment that blocks the electron transfer from PSII, indicating that the electrons accumulating in PSI in *pgr5* originate from PSII (Suorsa et al., 2012). Complementarily, it has been demonstrated that the *pgr5* phenotype can be alleviated by specifically down-regulating PSII (Tikkanen et al., 2014; Suorsa et al., 2016), suggesting that instead of accepting the electrons from PSI, PGR5 prevents them from entering PSI. A very liable possibility is that PGR5 modulates electron transfer from PSII to PSI – and thus possibly also CET – by controlling the proton conductivity of the thylakoid membrane. Indeed, *pgr5* behaves surprisingly similar to a *Nicotiana tabacum* mutant with decreased ATP synthase activity (Rott et al., 2011), and, in line with this, *pgr5* grown under fluctuating light, i.e. upon severe PSI photoinhibition, substantially upregulates the amount of ATP synthase (Suorsa et al., 2012). Moreover, it was recently demonstrated that the biophysical phenotype of a mutant with increased ATP synthase activity strikingly resembles that of *pgr5*, indicating that the behaviour of these mutants solely results from the impairment of the proton gradient (Kanazawa et al., 2017).

### 5.2.2 PGR5 protects PSI from photoinhibition by controlling the electron flow from PSII to PSI under excess light

The data presented in Papers II, III and IV calls into question any direct role of PGR5 as the major mediator of CET and demonstrates that, instead of CET, PGR5 is responsible for controlling the linear electron flow upon an increase in light intensity by preventing electrons from over-reducing PSI. Indeed, the dissection of the P700 oxidation kinetics in Paper IV showed that, upon a sudden increase in light intensity,

## DISCUSSION

the PGR5-dependent mechanism can be recruited in a few milliseconds, given that the mechanism is first activated by light, likely via lumen acidification (Figure 11). When active, PGR5 is able to decelerate electron transfer from PSII to PSI and to keep PSI oxidized even after a 70 % decrease in functional PSI (Figures 8 and 9A), suggesting that the function of PGR5 remains completely independent of the amount of functional PSI and is thus unlikely to be directly related to CET. Furthermore, as demonstrated by Figures 8 and 11, PGR5 is incapable of protecting PSI upon a sudden increase in light intensity if the electrons have already passed the photosynthetic control point at Cyt  $b_6f$ , confirming that the functional target of PGR5 is the donor side of PSI.

Paper IV demonstrated that the PGR5-dependent regulation of the proton gradient is of utmost importance in mitigating the consequences of PSI photoinhibition. An examination of the donor and acceptor side limitation of PSI (Figure 10A here and 5B in Paper IV) revealed that plants can compensate for the loss of PSI function by improving the electron transfer capacity of the remaining PSI and that this emergency measure is dependent on PGR5 under high light (Figure 9B). Indeed, as depicted in Figure 13, the photosynthetic control of Cyt  $b_6f$  allows the reduced plastocyanin and oxidized ferredoxin to diffuse from the damaged PSI centres and, as a result, to accelerate electron transfer through the functional centres. On the other hand, under light limiting conditions and without photosynthetic control plants seem to protect PSI by enhancing the capacity of the electron acceptors: the simultaneous high  $Y(ND)$  and low  $Y(NA)$  parameters under far-red and low actinic light (Figures 10A here and 5B in Paper IV) indicate that plants maintain a high ratio of stromal acceptors with respect to the luminal donors, which, in the absence of FLV proteins, likely protects PSI against any sudden burst of electrons under the naturally and constantly changing light intensity.

The western blots highlighted the importance of PGR5 in rebalancing the ETC after PSI photoinhibition: the photoinhibition treatment drastically upregulated the amount of PGR5 in WT and *ndho* (Figure 10B). The increased amount of PGR5 undoubtedly strengthens the proton gradient across the thylakoid membrane and, consequently, improves the regulation of ETC through photosynthetic control and thermal dissipation of excess excitation energy (Figure 13). Moreover, during the PSI repair, accelerating the synthesis of ATP is likely essential (Figure 13). Intriguingly, although the amount of PGR5 was upregulated under a PSI-limiting state, the amount of PGRL1 remained unaltered (Paper IV), indicating that PGR5 might also be able to function also independently of its membrane anchor. In fact, the enrichment of PGRL1 on the non-appressed membranes and the location of PGR5 in both appressed and non-appressed membranes (Hertle et al., 2013; Suorsa et al., 2014) suggest that the function of PGR5 is controlled by regulating the physical interaction between the proteins. This type of a dual function of PGR5

## DISCUSSION

would better agree with the hypothesis of PGRL1 as the antimycin A-sensitive CET pathway (Hertle et al., 2013). Indeed, unlike PGR5, PGRL1 is able to translocate electrons (Hertle et al., 2013), and the decreased amount of the possible PGRL1 mediated CET could explain some of the results obtained from *pgr5*. Nevertheless, even if PGR5 was required for the putative PGRL1 mediated CET, the data in Paper IV unequivocally indicates that the major role of PGR5 is the regulation of electron transfer from PSII to PSI – completely independently of the amount of functional PSI.

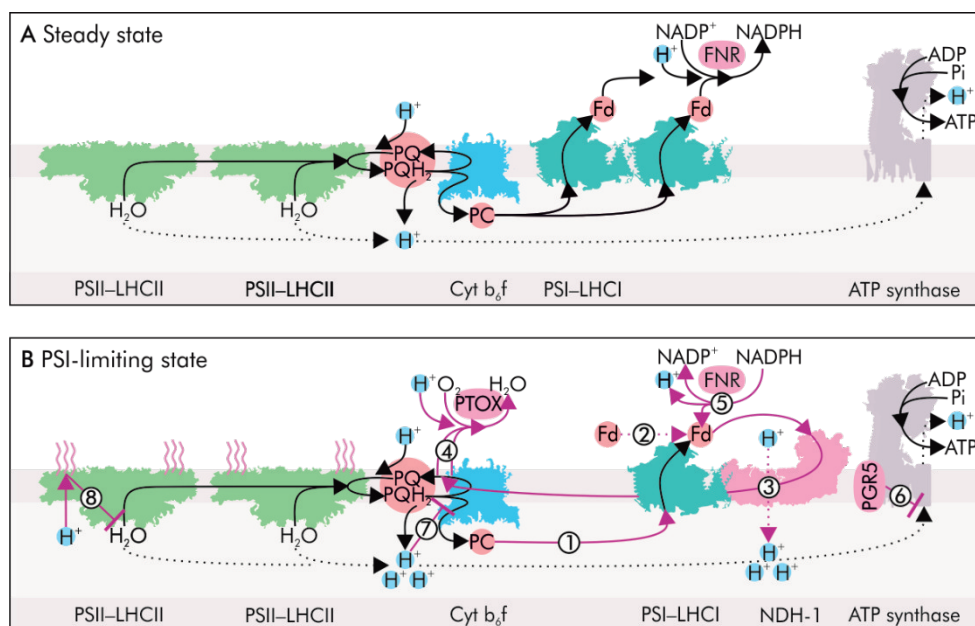


**Figure 13. Rebalancing the ETC after PSI photoinhibition.** **A.** Under steady-state conditions, photosynthetic light reactions are balanced in order to optimize the production of NADPH and ATP. **B.** The sudden loss of a fraction of PSI centres, however, severely disturbs the balance. The consequent relatively large pools of (1) reduced plastocyanin (PC) and (2) oxidized ferredoxin (Fd) are now utilized by the remaining functional PSI centres. (3) The electrons from Fd, on the other hand, are redirected into the PQ pool by NDH-1 and (4) from the PQ pool to  $O_2$  by PTOX. The action of PTOX not only scavenges the electrons deriving from PSI via NDH-1 but also prevents new electrons from entering PSI by draining them directly from the PQ pool. Importantly, NDH-1 and PTOX mediated chlororespiration strengthens the proton gradient: PTOX utilizes protons in the stroma and the electron transfer through NDH-1 is coupled to proton pumping from the chloroplast stroma into the thylakoid lumen. (5) In addition, it is possible that upon PSI inhibition, FNR starts to function in a reverse direction by oxidizing NADPH in order to produce reduced Fd for chlororespiration. (6) The enhanced proton gradient is maintained by the PGR5 protein and it (7) limits electron transfer from PSII to PSI, (8) induces the thermal dissipation of excess excitation energy and, finally, (9) accelerates the synthesis of ATP that is essential for PSI repair.

## DISCUSSION

### 5.2.3 NDH-1 and PTOX mitigate PSI photoinhibition by generating a proton gradient under light-limiting conditions

Intriguingly, the decrease in functional PSI centres lead to a clear upregulation of PTOX both in the WT and in the *pgr5* and *ndho* mutants (Figure 10B). The protein has also previously been reported to increase in amount in *pgr5* grown under both constant and fluctuating light conditions (Suorsa et al., 2012), suggesting a role for the protein as a safety valve under conditions that over-reduce PSI. Indeed, soon after its discovery (Cournac et al., 2000), PTOX was shown to restrict the electron flow from PSII to Cyt  $b_6/f$  during the slow activation of the carbon assimilation upon dark-to-light transition of plants (Joët et al., 2002). PTOX was, however, demonstrated to be unable to protect PSI from over-reduction upon a sudden increase in light intensity when grown under steady-state light conditions, suggesting that more drastic changes are needed for the protein to start properly oxidizing the PQ pool (Joët et al., 2002; Rosso et al., 2006). Based on the results by Suorsa et al., 2012 and those presented in Paper IV, such an activation signal could involve the photoinhibition of PSI.

In addition to PTOX, the *pgr5* mutant increased the amount of NDH-1 as a response to PSI inhibition (Figure 10B) and, in fact, similar concomitant upregulation has also been reported as a response to high light and high temperature i.e. in conditions leading to extreme reduction of the PQ pool (Quiles, 2006). As depicted in Figure 13, the simultaneous upregulation of NDH-1 and PTOX indicates an enhanced capacity of *pgr5* to oxidize the ETC through CET and chlororespiration: as the electron transfer through the still functional PSI centres increases, NDH-1 could safely redirect the electrons into the PQ pool for PTOX to reduce  $O_2$  with them. In addition to the direct oxidation of PSI by NDH-1 and the PQ pool by PTOX, the functioning of both NDH-1 and PTOX induces photosynthetic control and the thermal dissipation of excess excitation energy as well as improves the synthesis of ATP by decreasing the pH of the lumen (Figure 13). This results from the fact that electron transfer through NDH-1 is coupled to proton pumping from the chloroplast stroma into the thylakoid lumen and that the reduction of PQ to  $PQH_2$  as well as that of  $O_2$  to  $H_2O$  by PTOX consumes protons from the stroma.

Unlike PGR5, both NDH-1 and PTOX function independently of light activation, and thus *pgr5* is able to strengthen the proton gradient and the consequent photosynthetic control immediately on the onset of illumination. Likely due to the enhanced chlororespiration and the substantial proton pumping capacity of NDH-1, *pgr5* was able to keep PSI and thus the whole ETC relatively oxidized under low actinic light intensities (Figure 7) as well as under far-red light even after the most severe PSI inhibition (Figure 10A). It is also plausible that, in the PSI-limiting state, the chlororespiration capacity and consequently improved ATP synthesis are enhanced by reverse-functioning FNR that produces reduced ferredoxin even at the

## DISCUSSION

cost of NADPH, as illustrated in Figure 13. However, the dynamic distribution of FNR and the different forms of ferredoxin between the photosynthetic light reactions and chlororespiration remains to be elucidated.

Although PTOX was also seen upregulated in *ndho* as a response to PSI photoinhibition (Figure 10B), the simultaneous increase in the amount of PGR5 has likely enhanced the proton gradient under high light, masking the effect of PTOX and explaining the improvement in P700 oxidation (Figure 10A) and the alleviation of the acceptor side limitation (Figure 5B in Paper IV). These results from *ndho* are in line with previous reports (Joët et al., 2002; Rosso et al., 2006) showing that PTOX is capable of oxidizing the ETC only on the onset of illumination, and thus highlight the role of PGR5 as the major regulator under excess light.

## 6 Conclusions

The work in this thesis has provided novel details on the acclimation of photosynthetic light reactions to an increase in light intensity and the possible photoinhibition of PSI. It has elucidated how LHCB2 phosphorylation, photosynthetic control, thermal dissipation, cyclic electron transfer and chlororespiration together balance the photosynthetic light reactions in order to protect PSI from light-induced damage.

Paper I confirmed that only the STN7-dependent phosphorylation of the LHCB2 protein under low light enables the optimal excitation balance between the two photosystems by determining the attachment of PSI into the large megacomplex (Figure 12). Complementarily, it was shown that upon an increase in light intensity, PSI is protected from excess electrons by spatial separation of PSI from the megacomplex by TAP38/PPH1 phosphatase and, simultaneously, by an increase in the physical distance between PSII and Cyt b<sub>6</sub>f.

Papers II, III and IV cumulatively showed that the PGR5 protein protects PSI from over-reduction by modulating the photosynthetic control in a manner that is CET-independent. It was discovered in Paper IV that the function of PGR5 requires activation by light and that after activation, PGR5 can respond to an increase in light intensity in a few milliseconds. Paper IV also revealed that in the case of PSI photoinhibition, the ETC is rebalanced by NDH-1, PTOX and PGR5 (Figure 13). NDH-1 and PTOX mediated chlororespiration prevents the over-reduction of stromal acceptors under low light both by accepting electrons from PSI and by strengthening the proton gradient, but if the light intensity increases, PGR5 takes over the protection by enhancing the photosynthetic control of electron transfer from PSII to PSI. Furthermore, Paper IV demonstrated that plants are able to compensate for damaged PSI centres by accelerating electron transfer through the remaining functional ones by redistributing the mobile electron donors and acceptors.

## 7 Future perspectives

The ever-growing human population and ongoing climate change challenge the global production of food, feed and fuel. One way to improve photosynthetic production is to enhance the light reactions. However, based on the results of this thesis, special emphasis would have to be placed on avoiding the saturation of ETC and consequent PSI photoinhibition. For this reason, another more plausible way to improve production is to enhance the synthesis of organic compounds by photosynthesis. This could be attained by eliminating the restricting steps in photosynthetic light reactions and in the carbon assimilation. First, since the accumulating end products of photosynthesis inhibit their production via a negative feedback loop, larger sinks for the organic compounds would be essential. Second, the capacity of Rubisco to bind CO<sub>2</sub> should be improved in order to avoid wasteful photorespiration i.e. the reduction of O<sub>2</sub> instead of CO<sub>2</sub>. Third, once the carbon assimilation reactions would not limit the light reactions, the regulatory mechanisms controlling the electron flow from PSII to PSI could also be weakened in order to produce more ATP and NADPH for the carbon assimilation reactions. Alternatively, completely new metabolic routes could be designed to drain the electrons from the light reactions, which would again alleviate the effects of the strict regulatory mechanisms restricting the production of ATP and NADPH.

To be able to modify photosynthesis in any way, basic research is essential to understand how the light reactions are controlled under the natural environmental conditions as well as how they communicate with the rest of the chloroplast and the whole plant cell. While high-resolution imaging techniques are quite well developed, the fractionation of the thylakoid membrane remains as a valuable tool to investigate the dynamics of the photosynthetic light reactions. In addition to the fractionation of the thylakoid membrane, it is important to develop methods that retain the photosynthetic machinery as intact as possible in order to specifically target the regulatory mechanism of interest, as for instance was done with the deliberate PSI photoinhibitory treatment in Paper IV.

# Abbreviations

<b>ADP</b>	Adenosine diphosphate
<b>ATP</b>	Adenosine triphosphate
<b>B1-9</b>	BN bands
<b>BN</b>	Blue native
<b>BTH</b>	Bis-Tris buffer pH-adjusted with HCl
<b>CET</b>	Cyclic electron transfer
<b>Chl</b>	Chlorophyll
<b>CO<sub>2</sub></b>	Carbon dioxide
<b>Cyt b<sub>6</sub>f</b>	Cytochrome b <sub>6</sub> f complex
<b>DIG</b>	Digitonin
<b>DM</b>	Dodecyl maltoside
<b>EPR</b>	Electron paramagnetic resonance
<b>ETC</b>	Electron transfer chain
<b>ETR(I)</b>	Electron transfer through PSI, $[(P_M' - P')/P_M] \times \text{PPFD} \times 0.84 \times 0.5$
<b>ETR(II)</b>	Electron transfer through PSII, $[(FM' - F')/FM'] \times \text{PPFD} \times 0.84 \times 0.5$
<b>F'</b>	Fluorescence under light
<b>F<sub>0</sub></b>	Minimal fluorescence
<b>Fd</b>	Ferredoxin
<b>FeS</b>	Iron-sulphur
<b>FLV</b>	Flavodiiron
<b>F<sub>M</sub></b>	Maximal fluorescence after dark acclimation
<b>F<sub>M</sub>'</b>	Maximal fluorescence under light
<b>FNR</b>	Ferredoxin-NADPH-oxidoreductase
<b>FR</b>	Far-red light
<b>F<sub>V</sub></b>	Variable fluorescence, $F_M - F_0$
<b>GL</b>	Growth light
<b>H<sup>+</sup></b>	Proton
<b>H<sub>2</sub>O</b>	Water
<b>H<sub>2</sub>O<sub>2</sub></b>	Hydrogen peroxide
<b>HCl</b>	Hydrogen chloride
<b>HL</b>	High growth light, 500 mmol photons m <sup>-2</sup> s <sup>-1</sup>



## ABBREVIATIONS

<b>kD</b>	Kilodalton
<b>LHCI</b>	Light harvesting complex I
<b>LHCII</b>	Light harvesting complex II
<b>LL</b>	Low growth light, 50 photons m <sup>-2</sup> s <sup>-1</sup>
<b>L-LHCII</b>	Loosely bound LHCII
<b>MB</b>	Measuring beam
<b>ML</b>	Moderate growth light, 120 mmol photons m <sup>-2</sup> s <sup>-1</sup>
<b>M-LHCII</b>	Moderately bound LHCII
<b>NADP<sup>+</sup></b>	Oxidized nicotinamide adenine dinucleotide phosphate
<b>NADPH</b>	Reduced nicotinamide adenine dinucleotide phosphate
<b>NDH-1</b>	Type I NDH dehydrogenase
<b>NPQ</b>	Non-photochemical quenching of fluorescence
<b>O<sub>2</sub><sup>-</sup></b>	Superoxide anion
<b>OH<sup>-</sup></b>	Hydroxide anion
<b>P</b>	Pellet (Paper I) <b>or</b> P700 signal (Papers II–IV)
<b>P-</b>	Phosphoryl group on a protein
<b>P'</b>	P700 signal under light
<b>P<sup>o</sup></b>	P700 signal under light
<b>P680</b>	Primary electron donor of PSII
<b>P680*</b>	Excited P680
<b>P680<sup>+</sup></b>	Oxidized P680
<b>P700</b>	Primary electron donor of PSI
<b>P700*</b>	Excited P700
<b>P700<sup>+</sup></b>	Oxidized P700
<b>PAGE</b>	Polyacrylamide gel electrophoresis
<b>PAM</b>	Pulse amplitude modulated
<b>PC</b>	Plastocyanin
<b>PGR5</b>	PROTON GRADIENT REGULATION5
<b>PGRL1</b>	PROTON GRADIENT REGULATION LIKE 1
<b>pH</b>	Negative logarithm of H <sup>+</sup> concentration
<b>Phe</b>	Pheophytin
<b>P<sub>i</sub></b>	Inorganic phosphate
<b>PIT</b>	PSI photoinhibition treatment
<b>P<sub>M</sub></b>	Maximal P700 signal after dark acclimation
<b>P<sub>M</sub><sup>o</sup></b>	Maximal P700 signal under light
<b>PPFD</b>	Photosynthetic photon flux density
<b>PPH1</b>	PROTEIN PHOSPHATASE 1
<b>PQ</b>	Plastoquinone
<b>PQH<sub>2</sub></b>	Plastohydroquinone
<b>PSI</b>	Photosystem I

## ABBREVIATIONS

<b>PSII</b>	Photosystem II
<b>P-Thr</b>	Phosphothreonine
<b>PVDF</b>	Polyvinylidene fluoride
<b>Q</b>	Quinone
<b>S</b>	Supernatant, soluble digitonin fraction
<b>SDS</b>	Sodium dodecyl sulphate
<b>S-LHCII</b>	Strongly bound LHCII
<b>SP</b>	Saturating pulse
<b>STN7</b>	STATE TRANSITION7 kinase
<b>STN8</b>	STATE TRANSITION8 kinase
<b>TAP38</b>	THYLAKOID ASSOCIATED PHOSPHATASE of 38kD
<b>WT</b>	Wild type
<b>Y(NA)</b>	Acceptor side limitation of PSI, $P_M-P_M'/P_M$
<b>Y(ND)</b>	Donor side limitation of PSI, $P/P_M$
<b>Y<sub>D</sub></b>	Tyrosine D, an amino acid residue of D2 protein
<b>Y<sub>D</sub><sup>•</sup></b>	Tyrosine D radical of D2 protein
<b>Y<sub>Z</sub></b>	Tyrosine Z, an amino acid residue of D1 protein

## References

- Abrahams JP, Leslie AGW, Lutter R, Walker JE** (1994) Structure at 2.8 Å resolution of F1-ATPase from bovine heart mitochondria. *Nature* **370**: 621–628
- Akhtar P, Lingvay M, Kiss T, Deák R, Bóta A, Ughy B, Garab G, Lambrev PH** (2016) Excitation energy transfer between Light-harvesting complex II and Photosystem I in reconstituted membranes. *Biochim Biophys Acta BBA - Bioenerg* **1857**: 462–472
- Albertsson P-Å** (2001) A quantitative model of the domain structure of the photosynthetic membrane. *Trends Plant Sci* **6**: 349–354
- Alboresi A, Ballottari M, Hienerwadel R, Giacometti GM, Morosinotto T** (2009) Antenna complexes protect Photosystem I from Photoinhibition. *BMC Plant Biol* **9**: 71
- Allen JF, Bennett J, Steinback KE, Arntzen CJ** (1981) Chloroplast protein phosphorylation couples plastoquinone redox state to distribution of excitation energy between photosystems. *Nature* **291**: 25–29
- Anderson JM** (1986) Photoregulation of the Composition, Function, and Structure of Thylakoid Membranes. *Annu Rev Plant Physiol* **37**: 93–136
- Anderson JM** (1982) The role of chlorophyll-protein complexes in the function and structure of chloroplast thylakoids. *Mol Cell Biochem* **46**: 161–172
- Anderson JM, Boardman NK** (1966) Fractionation of the photochemical systems of photosynthesis I. Chlorophyll contents and photochemical activities of particles isolated from spinach chloroplasts. *Biochim Biophys Acta BBA - Biophys Photosynth* **112**: 403–421
- Andersson B, Anderson JM** (1980) Lateral heterogeneity in the distribution of chlorophyll-protein complexes of the thylakoid membranes of spinach chloroplasts. *Biochim Biophys Acta BBA - Bioenerg* **593**: 427–440
- Andreasson E, Svensson P, Weibull C, Albertsson P-Å** (1988) Separation and characterization of stroma and grana membranes — evidence for heterogeneity in antenna size of both Photosystem I and Photosystem II. *Biochim Biophys Acta BBA - Bioenerg* **936**: 339–350
- Armbruster U, Labs M, Pribil M, Viola S, Xu W, Scharfenberg M, Hertle AP, Rojahn U, Jensen PE, Rappaport F, et al** (2013) Arabidopsis CURVATURE THYLAKOID1 Proteins Modify Thylakoid Architecture by Inducing Membrane Curvature. *Plant Cell* **25**: 2661–2678
- Arnon DI, Allen MB, Whatley FR** (1954) Photosynthesis by Isolated Chloroplasts. *Nature* **174**: 394–396
- Aro E-M, Suorsa M, Rokka A, Allahverdiyeva Y, Paakkarinen V, Saleem A, Battchikova N, Rintamäki E** (2005) Dynamics of photosystem II: A proteomic approach to thylakoid protein complexes. *J Exp Bot* **56**: 347–356
- Aro E-M, Virgin I, Andersson B** (1993) Photoinhibition of Photosystem II. Inactivation, protein damage and turnover. *Biochim Biophys Acta BBA - Bioenerg* **1143**: 113–134
- Asada K** (1999) THE WATER-WATER CYCLE IN CHLOROPLASTS: Scavenging of Active Oxygens and Dissipation of Excess Photons. *Annu Rev Plant Physiol Plant Mol Biol* **50**: 601–639
- Austin JR, Staehelin LA** (2011) Three-Dimensional Architecture of Grana and Stroma Thylakoids of Higher Plants as Determined by Electron Tomography. *Plant Physiol* **155**: 1601–1611
- Baena-González E, Barbato R, Aro E-M** (1999) Role of phosphorylation in the repair cycle and oligomeric structure of photosystem II. *Planta* **208**: 196–204
- Barber J** (1980) An explanation for the relationship between salt-induced thylakoid stacking and the chlorophyll fluorescence changes associated with changes in spillover of energy from photosystem II to photosystem I. *FEBS Lett* **118**: 1–10

## REFERENCES

- Bellafore S, Barneche F, Peltier G, Rochaix J-D** (2005) State transitions and light adaptation require chloroplast thylakoid protein kinase STN7. *Nature* **433**: 892
- Bennett J, Steinback KE, Arntzen CJ** (1980) Chloroplast phosphoproteins: regulation of excitation energy transfer by phosphorylation of thylakoid membrane polypeptides. *Proc Natl Acad Sci* **77**: 5253–5257
- Bennoun P** (1982) Evidence for a respiratory chain in the chloroplast. *Proc Natl Acad Sci* **79**: 4352–4356
- Ben-Shem A, Frolow F, Nelson N** (2003) Crystal structure of plant photosystem I. *Nature* **426**: 630–635
- Benson SL, Maheswaran P, Ware MA, Hunter CN, Horton P, Jansson S, Ruban AV, Johnson MP** (2015) An intact light harvesting complex I antenna system is required for complete state transitions in *Arabidopsis*. *Nat Plants* **1**: 15176
- Bergantino E, Segalla A, Brunetta A, Teardo E, Rigoni F, Giacometti GM, Szabò I** (2003) Light- and pH-dependent structural changes in the PsbS subunit of photosystem II. *Proc Natl Acad Sci* **100**: 15265–15270
- Betterle N, Ballottari M, Zorzan S, Bianchi S de, Cazzaniga S, Dall’Osto L, Morosinotto T, Bassi R** (2009) Light-induced Dissociation of an Antenna Hetero-oligomer Is Needed for Non-photochemical Quenching Induction. *J Biol Chem* **284**: 15255–15266
- Bezouwen LS van, Caffarri S, Kale RS, Kouřil R, Thunnissen A-MWH, Oostergetel GT, Boekema EJ** (2017) Subunit and chlorophyll organization of the plant photosystem II supercomplex. *Nat Plants* **3**: 17080
- Boardman NK, Anderson JM** (1964) Isolation from Spinach Chloroplasts of Particles Containing Different Proportions of Chlorophyll a and Chlorophyll b and their Possible Role in the Light Reactions of Photosynthesis. *Nature* **203**: 166–167
- Boekema EJ, van Roon H, van Breemen JFL, Dekker JP** (1999) Supramolecular organization of photosystem II and its light-harvesting antenna in partially solubilized photosystem II membranes. *Eur J Biochem* **266**: 444–452
- Boekema EJ, Roon H van, Dekker JP** (1998) Specific association of photosystem II and light-harvesting complex II in partially solubilized photosystem II membranes. *FEBS Lett* **424**: 95–99
- Bonardi V, Pesaresi P, Becker T, Schleiff E, Wagner R, Pfannschmidt T, Jahns P, Leister D** (2005) Photosystem II core phosphorylation and photosynthetic acclimation require two different protein kinases. *Nature* **437**: 1179–1182
- Bos I, Bland KM, Tian L, Croce R, Frankel LK, van Amerongen H, Bricker TM, Wientjes E** (2017) Multiple LHCII antennae can transfer energy efficiently to a single Photosystem I. *Biochim Biophys Acta BBA - Bioenerg* **1858**: 371–378
- Breyton C, Nandha B, Johnson GN, Joliot P, Finazzi G** (2006) Redox Modulation of Cyclic Electron Flow around Photosystem I in C3 Plants. *Biochemistry* **45**: 13465–13475
- Burrows PA, Sazanov LA, Svab Z, Maliga P, Nixon PJ** (1998) Identification of a functional respiratory complex in chloroplasts through analysis of tobacco mutants containing disrupted plastid *ndh* genes. *EMBO J* **17**: 868–876
- Butler WL** (1972) On the Primary Nature of Fluorescence Yield Changes Associated with Photosynthesis. *Proc Natl Acad Sci* **69**: 3420–3422
- Carol P, Stevenson D, Bisanz C, Breitenbach J, Sandmann G, Mache R, Coupland G, Kuntz M** (1999) Mutations in the Arabidopsis Gene IMMUTANS Cause a Variegated Phenotype by Inactivating a Chloroplast Terminal Oxidase Associated with Phytoene Desaturation. *Plant Cell* **11**: 57–68
- Caspy I, Nelson N** (2018) Structure of the plant photosystem I. *Biochem Soc Trans* **BST20170299**
- Cazzaniga S, Li Z, Niyogi KK, Bassi R, Dall’Osto L** (2012) The Arabidopsis *szl1* Mutant Reveals a Critical Role of  $\beta$ -Carotene in Photosystem I Photoprotection. *Plant Physiol* **159**: 1745–1758
- Correa-Galvis V, Poschmann G, Melzer M, Stühler K, Jahns P** (2016) PsbS interactions involved in the activation of energy dissipation in *Arabidopsis*. *Nat Plants* **2**: 15225
- Cournac L, Josse E-M, Joët T, Rumeau D, Redding K, Kuntz M, Peltier G** (2000) Flexibility in photosynthetic electron transport: a newly identified chloroplast oxidase involved in chlororespiration. *Philos Trans R Soc Lond B Biol Sci* **355**: 1447–1454
- Crofts AR, Hong S, Ugulava N, Barquera B, Gennis R, Guergova-Kuras M, Berry EA** (1999) Pathways for proton release during ubiquinone oxidation by the bc1 complex. *Proc Natl Acad Sci* **96**: 10021–10026
- DalCorso G, Pesaresi P, Masiero S, Aseeva E, Schünemann D, Finazzi G, Joliot P, Barbato R, Leister D** (2008) A Complex Containing PGRL1 and PGR5 Is Involved in the Switch between

## REFERENCES

- Linear and Cyclic Electron Flow in Arabidopsis. *Cell* **132**: 273–285
- Danielsson R, Albertsson P-Å** (2009) Fragmentation and separation analysis of the photosynthetic membrane from spinach. *Biochim Biophys Acta BBA - Bioenerg* **1787**: 25–36
- Danielsson R, Albertsson P-Å, Mamedov F, Styring S** (2004) Quantification of photosystem I and II in different parts of the thylakoid membrane from spinach. *Biochim Biophys Acta BBA - Bioenerg* **1608**: 53–61
- Danielsson R, Suorsa M, Paakkari V, Albertsson P-Å, Styring S, Aro E-M, Mamedov F** (2006) Dimeric and Monomeric Organization of Photosystem II DISTRIBUTION OF FIVE DISTINCT COMPLEXES IN THE DIFFERENT DOMAINS OF THE THYLAKOID MEMBRANE. *J Biol Chem* **281**: 14241–14249
- Dau H** (1994) Molecular Mechanisms and Quantitative Models of Variable Photosystem II Fluorescence. *Photochem Photobiol* **60**: 1–23
- Daum B, Kühlbrandt W** (2011) Electron tomography of plant thylakoid membranes. *J Exp Bot* **62**: 2393–2402
- Dekker JP, Boekema EJ** (2005) Supramolecular organization of thylakoid membrane proteins in green plants. *Biochim Biophys Acta BBA - Bioenerg* **1706**: 12–39
- Demeter S, Govindjee** (1989) Thermoluminescence in plants. *Physiol Plant* **75**: 121–130
- Demmig-Adams B** (1990) Carotenoids and photoprotection in plants: A role for the xanthophyll zeaxanthin. *Biochim Biophys Acta BBA - Bioenerg* **1020**: 1–24
- Demmig-Adams B, Adams W** (1992) Photoprotection and Other Responses of Plants to High Light Stress. *Annu Rev Plant Physiol Plant Mol Biol* **43**: 599–626
- Depège N, Bellafiore S, Rochaix J-D** (2003) Role of Chloroplast Protein Kinase Stt7 in LHClI Phosphorylation and State Transition in *Chlamydomonas*. *Science* **299**: 1572–1575
- Dumas L, Chazaux M, Peltier G, Johnson X, Alric J** (2016) Cytochrome b6f function and localization, phosphorylation state of thylakoid membrane proteins and consequences on cyclic electron flow. *Photosynth Res* **129**: 307–320
- Duysens L, Sweers H** (1963) Mechanism of two photochemical reactions in algae as studied by means of fluorescence. *Plant Cell Physiol* **353–372**
- Endo T, Mil H, Shikanai T, Asada K** (1997) Donation of Electrons to Plastoquinone by NAD(P)H Dehydrogenase and by Ferredoxin-Quinone Reductase in Spinach Chloroplasts. *Plant Cell Physiol* **38**: 1272–1277
- Ettinger WF, Clear AM, Fanning KJ, Peck ML** (1999) Identification of a Ca<sup>2+</sup>/H<sup>+</sup> Antiport in the Plant Chloroplast Thylakoid Membrane. *Plant Physiol* **119**: 1379–1386
- Förster Th** (1946) Energiewanderung und Fluoreszenz. *Naturwissenschaften* **33**: 166–175
- Förster Th** (1948) Zwischenmolekulare Energiewanderung und Fluoreszenz. *Ann Phys* **437**: 55–75
- Foyer CH, Neukermans J, Queval G, Noctor G, Harbinson J** (2012) Photosynthetic control of electron transport and the regulation of gene expression. *J Exp Bot* **63**: 1637–1661
- Frenkel M, Bellafiore S, Rochaix J-D, Jansson S** (2007) Hierarchy amongst photosynthetic acclimation responses for plant fitness. *Physiol Plant* **129**: 455–459
- Fristedt R, Willig A, Granath P, Crèvecoeur M, Rochaix J-D, Vener AV** (2009) Phosphorylation of Photosystem II Controls Functional Macroscopic Folding of Photosynthetic Membranes in Arabidopsis. *Plant Cell* **21**: 3950–3964
- Genty B, Briantais J-M, Baker NR** (1989) The relationship between the quantum yield of photosynthetic electron transport and quenching of chlorophyll fluorescence. *Biochim Biophys Acta BBA - Gen Subj* **990**: 87–92
- Georgakopoulos JH, Argyroudi-Akoyunoglou JH** (1994) Release of a “light” thylakoid membrane fragment with high F730/F685 fluorescence emission ratio (77 K) by digitonin disruption from “low-salt”-destacked or phosphorylated thylakoids of pea. *J Photochem Photobiol B* **26**: 57–65
- Gerotto C, Alboresi A, Meneghesso A, Jokel M, Suorsa M, Aro E-M, Morosinotto T** (2016) Flavodiiron proteins act as safety valve for electrons in *Physcomitrella patens*. *Proc Natl Acad Sci* **113**: 12322–12327
- Gollan PJ, Lima-Melo Y, Tiwari A, Tikkanen M, Aro E-M** (2017) Interaction between photosynthetic electron transport and chloroplast sinks triggers protection and signalling important for plant productivity. *Phil Trans R Soc B* **372**: 20160390
- Goral TK, Johnson MP, Brain APR, Kirchhoff H, Ruban AV, Mullineaux CW** (2010) Visualizing the mobility and distribution of chlorophyll proteins in higher plant thylakoid membranes: effects of photoinhibition and protein phosphorylation. *Plant J Cell Mol Biol* **62**: 948–959

## REFERENCES

- Goral TK, Johnson MP, Duffy CDP, Brain APR, Ruban AV, Mullineaux CW** (2012) Light-harvesting antenna composition controls the macrostructure and dynamics of thylakoid membranes in Arabidopsis. *Plant J* **69**: 289–301
- Govindjee** (1995) Sixty-Three Years Since Kautsky: Chlorophyll a Fluorescence. *Funct Plant Biol* **22**: 131–160
- Govindjee, Shevela D, Björn LO** (2017) Evolution of the Z-scheme of photosynthesis: a perspective. *Photosynth Res* **133**: 5–15
- Grieco M, Suorsa M, Jajoo A, Tikkanen M, Aro E-M** (2015) Light-harvesting II antenna trimers connect energetically the entire photosynthetic machinery — including both photosystems II and I. *Biochim Biophys Acta BBA - Bioenerg* **1847**: 607–619
- Grieco M, Tikkanen M, Paakkarinen V, Kangasjärvi S, Aro E-M** (2012) Steady-state phosphorylation of light-harvesting complex II proteins preserves photosystem I under fluctuating white light. *Plant Physiol* **160**: 1896–1910
- Hamel P, Olive J, Pierre Y, Wollman F-A, Vitry C de** (2000) A New Subunit of Cytochrome b<sub>6</sub> f Complex Undergoes Reversible Phosphorylation upon State Transition. *J Biol Chem* **275**: 17072–17079
- Herbstová M, Tietz S, Kinzel C, Turkina MV, Kirchhoff H** (2012) Architectural switch in plant photosynthetic membranes induced by light stress. *Proc Natl Acad Sci* **109**: 20130–20135
- Hertle AP, Blunder T, Wunder T, Pesaresi P, Pribil M, Armbruster U, Leister D** (2013) PGRL1 is the elusive ferredoxin-plastoquinone reductase in photosynthetic cyclic electron flow. *Mol Cell* **49**: 511–523
- Holzwarth AR, Miloslavina Y, Nilkens M, Jahns P** (2009) Identification of two quenching sites active in the regulation of photosynthetic light-harvesting studied by time-resolved fluorescence. *Chem Phys Lett* **483**: 262–267
- Horton P, Black MT** (1981) Light-dependent quenching of chlorophyll fluorescence in pea chloroplasts induced by adenosine 5'-triphosphate. *Biochim Biophys Acta BBA - Bioenerg* **635**: 53–62
- Horton P, Ruban AV, Rees D, Pascal AA, Noctor G, Young AJ** (1991) Control of the light-harvesting function of chloroplast membranes by aggregation of the LHCII chlorophyll-protein complex. *FEBS Lett* **292**: 1–4
- Horton P, Wentworth M, Ruban A** (2005) Control of the light harvesting function of chloroplast membranes: The LHCII-aggregation model for non-photochemical quenching. *FEBS Lett* **579**: 4201–4206
- Hughes JL, Smith P, Pace R, Krausz E** (2006) Charge separation in photosystem II core complexes induced by 690–730 nm excitation at 1.7 K. *Biochim Biophys Acta BBA - Bioenerg* **1757**: 841–851
- Jansson S** (1994) The light-harvesting chlorophyll ab-binding proteins. *Biochim Biophys Acta BBA - Bioenerg* **1184**: 1–19
- Jansson S, Stefánsson H, Nyström U, Gustafsson P, Albertsson P-Å** (1997) Antenna protein composition of PS I and PS II in thylakoid sub-domains. *Biochim Biophys Acta BBA - Bioenerg* **1320**: 297–309
- Järvi S, Rantala M, Aro E-M** (2017) Oxygenic Photosynthesis – Light Reactions within the Frame of Thylakoid Architecture and Evolution. *Photosynth. Bioenerg. WORLD SCIENTIFIC*, pp 243–263
- Järvi S, Suorsa M, Aro E-M** (2015) Photosystem II repair in plant chloroplasts — Regulation, assisting proteins and shared components with photosystem II biogenesis. *Biochim Biophys Acta BBA - Bioenerg* **1847**: 900–909
- Järvi S, Suorsa M, Paakkarinen V, Aro E-M** (2011) Optimized native gel systems for separation of thylakoid protein complexes: novel super- and mega-complexes. *Biochem J* **439**: 207–214
- Joët T, Genty B, Josse E-M, Kuntz M, Cournac L, Peltier G** (2002) Involvement of a Plastid Terminal Oxidase in Plastoquinone Oxidation as Evidenced by Expression of the Arabidopsis thaliana Enzyme in Tobacco. *J Biol Chem* **277**: 31623–31630
- Joliot P, Johnson GN** (2011) Regulation of cyclic and linear electron flow in higher plants. *Proc Natl Acad Sci* **108**: 13317–13322
- Kallas T** (2012) Cytochrome b<sub>6</sub>f Complex at the Heart of Energy Transduction and Redox Signaling. *Photosynthesis. Springer, Dordrecht*, pp 501–560
- Kanazawa A, Ostendorf E, Kohzuma K, Hoh D, Strand DD, Sato-Cruz M, Savage L, Cruz JA, Fisher N, Froehlich JE, et al** (2017) Chloroplast ATP Synthase Modulation of the Thylakoid Proton Motive Force: Implications for Photosystem I and Photosystem II Photoprotection. *Front Plant Sci.* doi: 10.3389/fpls.2017.00719
- Kirchhoff H, Haferkamp S, Allen JF, Epstein DBA, Mullineaux CW** (2008) Protein Diffusion and Macromolecular Crowding in Thylakoid Membranes. *Plant Physiol* **146**: 1571–1578

## REFERENCES

- Kirchhoff H, Hall C, Wood M, Herbstová M, Tsabari O, Nevo R, Charuvi D, Shimoni E, Reich Z** (2011) Dynamic control of protein diffusion within the granal thylakoid lumen. *Proc Natl Acad Sci* **108**: 20248–20253
- Kirchhoff H, Li M, Puthiyaveetil S** (2017) Sublocalization of Cytochrome b6f Complexes in Photosynthetic Membranes. *Trends Plant Sci* **22**: 574–582
- Kiss AZ, Ruban AV, Horton P** (2008) The PsbS Protein Controls the Organization of the Photosystem II Antenna in Higher Plant Thylakoid Membranes. *J Biol Chem* **283**: 3972–3978
- Kitajima M, Butler WL** (1975) Quenching of chlorophyll fluorescence and primary photochemistry in chloroplasts by dibromothymoquinone. *Biochim Biophys Acta BBA - Bioenerg* **376**: 105–115
- Klughammer C, Schreiber U** (2008) Saturation Pulse method for assessment of energy conversion in PS I. *PAM Appl Notes* **1**: 11–14
- Klughammer C, Schreiber U** (1994) An improved method, using saturating light pulses, for the determination of photosystem I quantum yield via P700+ -absorbance changes at 830 nm. *Planta* **192**: 261–268
- Kouřil R, Dekker JP, Boekema EJ** (2012) Supramolecular organization of photosystem II in green plants. *Biochim Biophys Acta BBA - Bioenerg* **1817**: 2–12
- Kouřil R, Oostergetel GT, Boekema EJ** (2011) Fine structure of granal thylakoid membrane organization using cryo electron tomography. *Biochim Biophys Acta BBA - Bioenerg* **1807**: 368–374
- Krumova SB, Várkonyi Zs, Lambrev PH, Kovács L, Todinova SJ, Busheva MC, Taneva SG, Garab G** (2014) Heat- and light-induced detachment of the light-harvesting antenna complexes of photosystem I in isolated stroma thylakoid membranes. *J Photochem Photobiol B* **137**: 4–12
- Kudoh H, Sonoike K** (2002) Irreversible damage to photosystem I by chilling in the light: cause of the degradation of chlorophyll after returning to normal growth temperature. *Planta* **215**: 541–548
- Kyle DJ, Kuang T-Y, Watson JL, Arntzen CJ** (1984) Movement of a sub-population of the light harvesting complex (LHCII) from grana to stroma lamellae as a consequence of its phosphorylation. *Biochim Biophys Acta BBA - Bioenerg* **765**: 89–96
- Kyle DJ, Staehelin LA, Arntzen CJ** (1983) Lateral mobility of the light-harvesting complex in chloroplast membranes controls excitation energy distribution in higher plants. *Arch Biochem Biophys* **222**: 527–541
- Laughlin TG, Bayne AN, Trempe J-F, Savage DF, Davies KM** (2019) Structure of the complex I-like molecule NDH of oxygenic photosynthesis. *Nature* **566**: 411
- Lennon AM, Prommeenate P, Nixon PJ** (2003) Location, expression and orientation of the putative chlororespiratory enzymes, Ndh and IMMUTANS, in higher-plant plastids. *Planta* **218**: 254–260
- Li X-P, Björkman O, Shih C, Grossman AR, Rosenquist M, Jansson S, Niyogi KK** (2000) A pigment-binding protein essential for regulation of photosynthetic light harvesting. *Nature* **403**: 391–395
- Li X-P, Gilmore AM, Caffarri S, Bassi R, Golan T, Kramer D, Niyogi KK** (2004) Regulation of Photosynthetic Light Harvesting Involves Intrathylakoid Lumen pH Sensing by the PsbS Protein. *J Biol Chem* **279**: 22866–22874
- Lima-Melo Y, Gollan PJ, Tikkanen M, Silveira JAG, Aro E-M** (2018) Consequences of photosystem-I damage and repair on photosynthesis and carbon use in *Arabidopsis thaliana*. *Plant J*. doi: 10.1111/tpl.14177
- Lunde C, Jensen PE, Haldrup A, Knoetzel J, Scheller HV** (2000) The PSI-H subunit of photosystem I is essential for state transitions in plant photosynthesis. *Nature* **408**: 613–615
- Miller KR, Staehelin LA** (1976) Analysis of the thylakoid outer surface. Coupling factor is limited to unstacked membrane regions. *J Cell Biol* **68**: 30–47
- Mitchell P** (1966) Chemiosmotic Coupling in Oxidative and Photosynthetic Phosphorylation. *Biol Rev* **41**: 445–501
- Miyake C, Miyata M, Shinzaki Y, Tomizawa K** (2005) CO<sub>2</sub> Response of Cyclic Electron Flow around PSI (CEF-PSI) in Tobacco Leaves—Relative Electron fluxes through PSI and PSII Determine the Magnitude of Non-photochemical Quenching (NPQ) of Chl Fluorescence. *Plant Cell Physiol* **46**: 629–637
- Mukerji I (University of C, Sauer K)** (1989) Temperature-dependent steady-state and picosecond kinetic fluorescence measurements of a photosystem I preparation from spinach. *Plant Biol. USA*
- Munekage Y, Hojo M, Meurer J, Endo T, Tasaka M, Shikanai T** (2002) PGR5 Is Involved in Cyclic Electron Flow around Photosystem I and Is Essential for Photoprotection in *Arabidopsis*. *Cell* **110**: 361–371

## REFERENCES

- Murphy DJ** (1986) The molecular organisation of the photosynthetic membranes of higher plants. *Biochim Biophys Acta BBA - Rev Biomembr* **864**: 33–94
- Mustárdy L, Buttle K, Steinbach G, Garab G** (2008) The Three-Dimensional Network of the Thylakoid Membranes in Plants: Quasihelical Model of the Granum-Stroma Assembly. *Plant Cell* **20**: 2552–2557
- Mustárdy L, Garab G** (2003) Granum revisited. A three-dimensional model – where things fall into place. *Trends Plant Sci* **8**: 117–122
- Paolillo DJ** (1970) The Three-Dimensional Arrangement of Intergranal Lamellae in Chloroplasts. *J Cell Sci* **6**: 243–253
- Peng L, Fukao Y, Fujiwara M, Takami T, Shikanai T** (2009) Efficient operation of NAD(P)H dehydrogenase requires supercomplex formation with photosystem I via minor LHCl in Arabidopsis. *Plant Cell* **21**: 3623–3640
- Pribil M, Pesaresi P, Hertle A, Barbato R, Leister D** (2010) Role of plastid protein phosphatase TAP38 in LHCII dephosphorylation and thylakoid electron flow. *PLoS Biol* **8**: e1000288
- Quiles MJ** (2006) Stimulation of chlororespiration by heat and high light intensity in oat plants. *Plant Cell Environ* **29**: 1463–1470
- Rantala M, Lehtimäki N, Aro E-M, Suorsa M** (2016) Downregulation of TAP38/PPH1 enables LHCII hyperphosphorylation in Arabidopsis mutant lacking LHCII docking site in PSI. *FEBS Lett* **590**: 787–794
- Rantala M, Tikkanen M, Aro E** (2017) Proteomic characterization of hierarchical megacomplex formation in Arabidopsis thylakoid membrane. *Plant J* **92**: 951–962
- Rintamäki E, Kettunen R, Aro E-M** (1996) Differential D1 Dephosphorylation in Functional and Photodamaged Photosystem II Centers DEPHOSPHORYLATION IS A PREREQUISITE FOR DEGRADATION OF DAMAGED D1. *J Biol Chem* **271**: 14870–14875
- Rintamäki E, Martinsuo P, Pursiheimo S, Aro E-M** (2000) Cooperative regulation of light-harvesting complex II phosphorylation via the plastoquinol and ferredoxin-thioredoxin system in chloroplasts. *Proc Natl Acad Sci* **97**: 11644–11649
- Rintamäki E, Salonen M, Suoranta U-M, Carlberg I, Andersson B, Aro E-M** (1997) Phosphorylation of Light-harvesting Complex II and Photosystem II Core Proteins Shows Different Irradiance-dependent Regulation in Vivo APPLICATION OF PHOSPHOTHREONINE ANTIBODIES TO ANALYSIS OF THYLAKOID PHOSPHOPROTEINS. *J Biol Chem* **272**: 30476–30482
- Rokka A, Suorsa M, Saleem A, Battchikova N, Aro E-M** (2005) Synthesis and assembly of thylakoid protein complexes: multiple assembly steps of photosystem II. *Biochem J* **388**: 159–168
- Rosso D, Ivanov AG, Fu A, Geisler-Lee J, Hendrickson L, Geisler M, Stewart G, Krol M, Hurry V, Rodermeil SR, et al** (2006) IMMUTANS Does Not Act as a Stress-Induced Safety Valve in the Protection of the Photosynthetic Apparatus of Arabidopsis during Steady-State Photosynthesis. *Plant Physiol* **142**: 574–585
- Rott M, Martins NF, Thiele W, Lein W, Bock R, Kramer DM, Schöttler MA** (2011) ATP Synthase Repression in Tobacco Restricts Photosynthetic Electron Transport, CO<sub>2</sub> Assimilation, and Plant Growth by Overacidification of the Thylakoid Lumen. *Plant Cell* **23**: 304–321
- Rozak PR, Seiser RM, Wacholtz WF, Wise RR** (2002) Rapid, reversible alterations in spinach thylakoid appression upon changes in light intensity. *Plant Cell Environ* **25**: 421–429
- Rumberg B, Siggel U** (1969) pH changes in the inner phase of the thylakoids during photosynthesis. *Naturwissenschaften* **56**: 130–132
- Rumeau D, Bécuwe-Linka N, Beyly A, Louwagie M, Garin J, Peltier G** (2005) New Subunits NDH-M, -N, and -O, Encoded by Nuclear Genes, Are Essential for Plastid Ndh Complex Functioning in Higher Plants. *Plant Cell* **17**: 219–232
- Rumeau D, Peltier G, Cournac L** (2007) Chlororespiration and cyclic electron flow around PSI during photosynthesis and plant stress response. *Plant Cell Environ* **30**: 1041–1051
- Samol I, Shapiguzov A, Ingelsson B, Fucile G, Crèvecoeur M, Vener AV, Rochaix J-D, Goldschmidt-Clermont M** (2012) Identification of a Photosystem II Phosphatase Involved in Light Acclimation in Arabidopsis. *Plant Cell* **24**: 2596–2609
- Schreiber U, Schliwa U, Bilger W** (1986) Continuous recording of photochemical and non-photochemical chlorophyll fluorescence quenching with a new type of modulation fluorometer. *Photosynth Res* **10**: 51–62
- Shapiguzov A, Ingelsson B, Samol I, Andres C, Kessler F, Rochaix J-D, Vener AV, Goldschmidt-Clermont M** (2010) The PPH1 phosphatase is specifically involved in LHCII dephosphorylation and state transitions in



## REFERENCES

- Arabidopsis. Proc Natl Acad Sci U S A **107**: 4782–4787
- Shuvalov VA, Nuijs AM, van Gorkom HJ, Smit HWJ, Duysens LNM** (1986) Picosecond absorbance changes upon selective excitation of the primary electron donor P-700 in Photosystem I. Biochim Biophys Acta BBA - Bioenerg **850**: 319–323
- Sirpiö S, Allahverdiyeva Y, Holmström M, Khrouchtchova A, Haldrup A, Battchikova N, Aro E-M** (2009) Novel Nuclear-encoded Subunits of the Chloroplast NAD(P)H Dehydrogenase Complex. J Biol Chem **284**: 905–912
- Sonoike K** (1996) Degradation of psaB gene product, the reaction center subunit of photosystem I, is caused during photoinhibition of photosystem I: possible involvement of active oxygen species. Plant Sci **115**: 157–164
- Sonoike K** (2011) Photoinhibition of photosystem I. Physiol Plant **142**: 56–64
- Sonoike K, Kamo M, Hihara Y, Hiyama T, Enami I** (1997) The mechanism of the degradation of psaB gene product, one of the photosynthetic reaction center subunits of Photosystem I, upon photoinhibition. Photosynth Res **53**: 55–63
- Spetea C, Schoefs B** (2010) Solute transporters in plant thylakoid membranes. Commun Integr Biol **3**: 122–129
- Standfuss J, Scheltinga ACT van, Lamborghini M, Kühlbrandt W** (2005) Mechanisms of photoprotection and nonphotochemical quenching in pea light-harvesting complex at 2.5 Å resolution. EMBO J **24**: 919–928
- Stiehl HH, Witt HT** (1969) Quantitative Treatment of the Function of Plastoquinone in Photosynthesis. Z Für Naturforschung B **24**: 1588–1598
- Strand DD, Livingston AK, Satoh-Cruz M, Koepke T, Enlow HM, Fisher N, Froehlich JE, Cruz JA, Minhas D, Hixson KK, et al** (2017) Defects in the Expression of Chloroplast Proteins Leads to H<sub>2</sub>O<sub>2</sub> Accumulation and Activation of Cyclic Electron Flow around Photosystem I. Front Plant Sci. doi: 10.3389/fpls.2016.02073
- Stroebel D, Choquet Y, Popot J-L, Picot D** (2003) An atypical haem in the cytochrome *b<sub>6</sub>f* complex. Nature **426**: 413–418
- Su X, Ma J, Wei X, Cao P, Zhu D, Chang W, Liu Z, Zhang X, Li M** (2017) Structure and assembly mechanism of plant C2S2M2-type PSII-LHCII supercomplex. Science **357**: 815–820
- Suorsa M, Järvi S, Grieco M, Nurmi M, Pietrzykowska M, Rantala M, Kangasjärvi S, Paakkari V, Tikkanen M, Jansson S, et al** (2012) PROTON GRADIENT REGULATION5 Is Essential for Proper Acclimation of Arabidopsis Photosystem I to Naturally and Artificially Fluctuating Light Conditions. Plant Cell **24**: 2934–2948
- Suorsa M, Rantala M, Danielsson R, Järvi S, Paakkari V, Schröder WP, Styring S, Mamedov F, Aro E-M** (2014) Dark-adapted spinach thylakoid protein heterogeneity offers insights into the photosystem II repair cycle. Biochim Biophys Acta BBA - Bioenerg **1837**: 1463–1471
- Suorsa M, Rantala M, Mamedov F, Lespinasse M, Trotta A, Grieco M, Vuorio E, Tikkanen M, Järvi S, Aro E** (2015) Light acclimation involves dynamic re-organization of the pigment–protein megacomplexes in non-appressed thylakoid domains. Plant J **84**: 360–373
- Suorsa M, Rossi F, Tadini L, Labs M, Colombo M, Jahns P, Kater MM, Leister D, Finazzi G, Aro E-M, et al** (2016) PGR5-PGRL1-Dependent Cyclic Electron Transport Modulates Linear Electron Transport Rate in Arabidopsis thaliana. Mol Plant **9**: 271–288
- Tagawa K, Tsujimoto HY, Arnon DI** (1963) Role of Chloroplast Ferredoxin in the Energy Conversion Process of Photosynthesis. Proc Natl Acad Sci **49**: 567–572
- Terashima I, Funayama S, Sonoike K** (1994) The site of photoinhibition in leaves of Cucumis sativus L. at low temperatures is photosystem I, not photosystem II. Planta **193**: 300–306
- Tikkanen M, Grebe S** (2018) Switching off photoprotection of photosystem I – a novel tool for gradual PSI photoinhibition. Physiol Plant **162**: 156–161
- Tikkanen M, Mekala NR, Aro E-M** (2014) Photosystem II photoinhibition-repair cycle protects Photosystem I from irreversible damage. Biochim Biophys Acta BBA - Bioenerg **1837**: 210–215
- Tikkanen M, Nurmi M, Kangasjärvi S, Aro E-M** (2008) Core protein phosphorylation facilitates the repair of photodamaged photosystem II at high light. Biochim Biophys Acta BBA - Bioenerg **1777**: 1432–1437
- Tikkanen M, Piippo M, Suorsa M, Sirpiö S, Mulo M, Vainonen J, Vener A, Allahverdiyeva Y, Aro E-M** (2006) State transitions revisited—a buffering system for dynamic low light acclimation of Arabidopsis. Plant Mol Biol **62**: 779
- Tjus SE, Møller BL, Scheller HV** (1999) Photoinhibition of Photosystem I damages both reaction centre proteins PSI-A and PSI-B and

## REFERENCES

- acceptor-side located small Photosystem I polypeptides. *Photosynth Res* **60**: 75–86
- Trotta A, Suorsa M, Rantala M, Lundin B, Aro E-M** (2016) Serine and threonine residues of plant STN7 kinase are differentially phosphorylated upon changing light conditions and specifically influence the activity and stability of the kinase. *Plant J* **87**: 484–494
- Tyystjärvi E, Aro EM** (1996) The rate constant of photoinhibition, measured in lincomycin-treated leaves, is directly proportional to light intensity. *Proc Natl Acad Sci* **93**: 2213–2218
- Umena Y, Kawakami K, Shen J-R, Kamiya N** (2011) Crystal structure of oxygen-evolving photosystem II at a resolution of 1.9 Å. *Nature* **473**: 55
- Vainonen JP, Hansson M, Vener AV** (2005) STN8 Protein Kinase in *Arabidopsis thaliana* Is Specific in Phosphorylation of Photosystem II Core Proteins. *J Biol Chem* **280**: 33679–33686
- Vener AV, van Kan PJM, Rich PR, Ohad I, Andersson B** (1997) Plastoquinol at the quinol oxidation site of reduced cytochrome *b<sub>f</sub>* mediates signal transduction between light and protein phosphorylation: Thylakoid protein kinase deactivation by a single-turnover flash. *Proc Natl Acad Sci* **94**: 1585–1590
- Volkmer T, Schneider D, Bernát G, Kirchhoff H, Wenk S-O, Rögner M** (2007) Ssr2998 of *Synechocystis* sp. PCC 6803 Is Involved in Regulation of Cyanobacterial Electron Transport and Associated with the Cytochrome *b<sub>6</sub>f* Complex. *J Biol Chem* **282**: 3730–3737
- Wei X, Su X, Cao P, Liu X, Chang W, Li M, Zhang X, Liu Z** (2016) Structure of spinach photosystem II–LHCII supercomplex at 3.2 Å resolution. *Nature* **534**: 69–74
- Wientjes E, van Amerongen H, Croce R** (2013a) LHCII is an antenna of both photosystems after long-term acclimation. *Biochim Biophys Acta BBA - Bioenerg* **1827**: 420–426
- Wientjes E, Drop B, Kouřil R, Boekema EJ, Croce R** (2013b) During State 1 to State 2 Transition in *Arabidopsis thaliana*, the Photosystem II Supercomplex Gets Phosphorylated but Does Not Disassemble. *J Biol Chem* **288**: 32821–32826
- Willig A, Shapiguzov A, Goldschmidt-Clermont M, Rochaix J-D** (2011) The Phosphorylation Status of the Chloroplast Protein Kinase STN7 of *Arabidopsis* Affects Its Turnover. *Plant Physiol* **157**: 2102–2107
- Wittig I, Braun H-P, Schagger H** (2006) Blue native PAGE. *Nat Protoc* **1**: 418–428
- Wood WH, Barnett SFH, Flannery S, Hunter CN, Johnson MP** (2019) Dynamic thylakoid stacking is regulated by LHCII phosphorylation but not its interaction with photosystem I. *Plant Physiol* pp.00503.2019
- Wu D, Wright DA, Wetzel C, Voytas DF, Rodermeier S** (1999) The IMMUTANS Variegation Locus of *Arabidopsis* Defines a Mitochondrial Alternative Oxidase Homolog That Functions during Early Chloroplast Biogenesis. *Plant Cell* **11**: 43–55
- Wunder T, Xu W, Liu Q, Wanner G, Leister D, Pribil M** (2013) The major thylakoid protein kinases STN7 and STN8 revisited: effects of altered STN8 levels and regulatory specificities of the STN kinases. *Front Plant Sci*. doi: 10.3389/fpls.2013.00417
- Yamamoto H, Peng L, Fukao Y, Shikanai T** (2011) An Src Homology 3 Domain-Like Fold Protein Forms a Ferredoxin Binding Site for the Chloroplast NADH Dehydrogenase-Like Complex in *Arabidopsis*. *Plant Cell* **23**: 1480–1493
- Yamori W, Shikanai T** (2016) Physiological Functions of Cyclic Electron Transport Around Photosystem I in Sustaining Photosynthesis and Plant Growth. *Annu Rev Plant Biol* **67**: 81–106
- Yamori W, Shikanai T, Makino A** (2015) Photosystem I cyclic electron flow via chloroplast NADH dehydrogenase-like complex performs a physiological role for photosynthesis at low light. *Sci Rep* **5**: 13908
- Yokono M, Akimoto S** (2018) Energy transfer and distribution in photosystem super/megacomplexes of plants. *Curr Opin Biotechnol* **54**: 50–56
- Yokono M, Takabayashi A, Akimoto S, Tanaka A** (2015) A megacomplex composed of both photosystem reaction centres in higher plants. *Nat Commun* **6**: 6675
- Zhang L, Paakkarinen V, Wijk KJ van, Aro E-M** (1999) Co-translational Assembly of the D1 Protein into Photosystem II. *J Biol Chem* **274**: 16062–16067
- Zhang S, Scheller HV** (2004) Photoinhibition of Photosystem I at Chilling Temperature and Subsequent Recovery in *Arabidopsis thaliana*. *Plant Cell Physiol* **45**: 1595–1602



*Annales Universitatis Turkuensis*



**UNIVERSITY  
OF TURKU**

ISBN 978-951-29-7734-5 (PRINT)

ISBN 978-951-29-7735-2 (PDF)

ISSN 0082-7002 (Print)

ISSN 2343-3175 (Online)